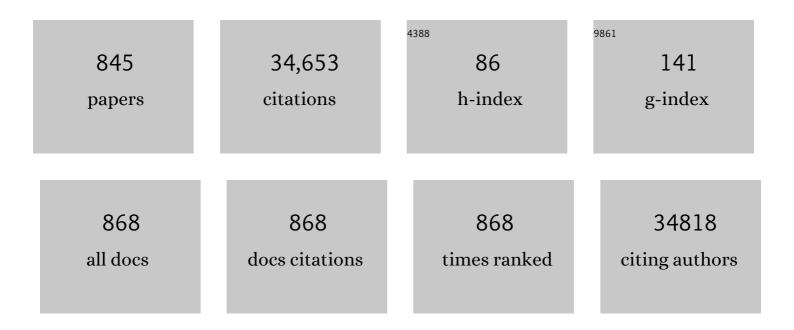


## List of Publications by Year in descending order

Source: https://exaly.com/author-pdf/137333/publications.pdf Version: 2024-02-01



ΙΙΔΝΙ ΧΙΙ

#	Article	IF	CITATIONS
1	Improving xylo-oligosaccharides yield from corn stalk with stepwise enzymolysis. Biomass Conversion and Biorefinery, 2023, 13, 3863-3869.	4.6	2
2	Intellectual capital efficiency and firms' financial performance based on business life cycle. Journal of Intellectual Capital, 2023, 24, 653-682.	5.4	3
3	The interrelationship between intellectual capital and firm performance: evidence from China's manufacturing sector. Journal of Intellectual Capital, 2022, 23, 313-341.	5.4	42
4	Organophosphate esters in sediment from Taihu Lake, China: Bridging the gap between riverine sources and lake sinks. Frontiers of Environmental Science and Engineering, 2022, 16, 1.	6.0	8
5	Arginine methylation in the epithelialâ€toâ€mesenchymal transition. FEBS Journal, 2022, 289, 7292-7303.	4.7	7
6	Does R&D investment moderate the relationship between the COVID-19 pandemic and firm performance in China's high-tech industries? Based on DuPont components. Technology Analysis and Strategic Management, 2022, 34, 1464-1478.	3.5	16
7	Single-atom Co embedded in BCN matrix to achieve 100% conversion of peroxymonosulfate into singlet oxygen. Applied Catalysis B: Environmental, 2022, 300, 120759.	20.2	78
8	Atomic-dispersed copper simultaneously achieve high-efficiency removal and high-value-added conversion to ammonia of nitrate in sewage. Journal of Hazardous Materials, 2022, 424, 127319.	12.4	43
9	Synergistic effect of acidity balance and hydrothermal pretreatment severity on alkali extraction of hemicelluloses from corn stalk. Biomass Conversion and Biorefinery, 2022, 12, 459-468.	4.6	8
10	Response of PM2.5-bound elemental species to emission variations and associated health risk assessment during the COVID-19 pandemic in a coastal megacity. Journal of Environmental Sciences, 2022, 122, 115-127.	6.1	11
11	Vertical profile and assessment of soil pollution from a typical coking plant by suspect screening and non-target screening using GC/QTOF-MS. Science of the Total Environment, 2022, 810, 151278.	8.0	6
12	Extracting Inherent Model Structures and Identifying Parameters of Time-Varying Systems Using Local Linear Neuro-Fuzzy Networks. IEEE Transactions on Fuzzy Systems, 2022, 30, 233-247.	9.8	6
13	Stereoselective profiling of methamphetamine in a full-scale wastewater treatment plant and its biotransformation in the activated sludge batch experiments. Water Research, 2022, 209, 117908.	11.3	1
14	Experimental Study on Uniaxial Compression Behavior of Fissured Loess Before and After Vibration. International Journal of Geomechanics, 2022, 22, .	2.7	17
15	Association between air pollution and outpatient visits for allergic rhinitis: Effect modification by ambient temperature and relative humidity. Science of the Total Environment, 2022, 821, 152960.	8.0	14
16	A novel plant-internal route of recycling sulfur from the flue gas desulfurization (FGD) ash through sintering process: From lab-scale principles to industrial practices. Journal of Environmental Chemical Engineering, 2022, 10, 106957.	6.7	5
17	Fabrication and long persistent luminescence of Ce3+-Cr3+ co-doped yttrium aluminum gallium garnet transparent ceramics. Journal of Rare Earths, 2022, 40, 1699-1705.	4.8	7
18	Singleâ€cell Raman microspectroscopyâ€based assessment of three intracanal disinfectants' effect on <scp><i>Enterococcus faecalis</i></scp> . Journal of Raman Spectroscopy, 2022, 53, 902-910.	2.5	5

#	Article	IF	CITATIONS
19	Primordial mimicry induces morphological change in Escherichia coli. Communications Biology, 2022, 5, 24.	4.4	7
20	Tunable broadband low-frequency band gap of multiple-layer metastructure induced by time-delayed vibration absorbers. Nonlinear Dynamics, 2022, 107, 1903-1918.	5.2	8
21	Species-resolved sequencing of low-biomass or degraded microbiomes using 2bRAD-M. Genome Biology, 2022, 23, 36.	8.8	31
22	Influence of the Residual Iron on the Erosion of Carbon Bricks in a 4000 m3 Blast Furnace Hearth: From the Measured Properties to the Proposed Mechanisms. Metallurgical and Materials Transactions B: Process Metallurgy and Materials Processing Science, 2022, 53, 931.	2.1	3
23	Triadimefon in aquatic environments: occurrence, fate, toxicity, and ecological risk. Environmental Sciences Europe, 2022, 34, .	5.5	10
24	Deep-red to near-infrared luminescence from Eu <sup>2+</sup> -trapped exciton states in YSiO <sub>2</sub> N. Physical Chemistry Chemical Physics, 2022, 24, 4348-4357.	2.8	2
25	High-Throughput Continuous-Flow Separation in a Micro Free-Flow Electrophoresis Glass Chip Based on Laser Microfabrication. Sensors, 2022, 22, 1124.	3.8	3
26	Unraveling electron liberation from Bi2+ for designing Bi3+-based afterglow phosphor for anti-counterfeiting and flexible X-ray imaging. Chemical Engineering Journal, 2022, 435, 135038.	12.7	32
27	The Impact of Intellectual Capital on Bank Profitability during COVID-19: A Comparison with China and Pakistan. Complexity, 2022, 2022, 1-10.	1.6	14
28	Cross-Regional Analysis of the Aging Phenomenon of Biomedical Scholars. Lecture Notes in Computer Science, 2022, , 244-254.	1.3	0
29	Does Intellectual Capital Affect Financial Leverage of Chinese Agricultural Companies? Exploring the Role of Firm Profitability. Sustainability, 2022, 14, 2682.	3.2	8
30	Assessing Efficacy of Clinical Disinfectants for Pathogenic Fungi by Single-Cell Raman Microspectroscopy. Frontiers in Cellular and Infection Microbiology, 2022, 12, 772378.	3.9	1
31	Three-Dimensional Large-Scale Fused Silica Microfluidic Chips Enabled by Hybrid Laser Microfabrication for Continuous-Flow UV Photochemical Synthesis. Micromachines, 2022, 13, 543.	2.9	8
32	IS TOO MUCH A GOOD THING? THE NON-LINEAR RELATIONSHIP BETWEEN INTELLECTUAL CAPITAL AND FINANCIAL COMPETITIVENESS IN THE CHINESE AUTOMOTIVE INDUSTRY. Journal of Business Economics and Management, 2022, 23, 773-796.	2.4	4
33	Self-/mutual-symmetric rhythms and their coexistence in a delayed half-center oscillator of the CPG neural system. Nonlinear Dynamics, 2022, 108, 2595-2609.	5.2	13
34	Exploring a blue-light-sensing transcription factor to double the peak productivity of oil in Nannochloropsis oceanica. Nature Communications, 2022, 13, 1664.	12.8	12
35	Atmospheric Processing at the Seaâ€Land Interface Over the South China Sea: Secondary Aerosol Formation, Aerosol Acidity, and Role of Sea Salts. Journal of Geophysical Research D: Atmospheres, 2022, 127, .	3.3	7
36	Effect of dopant concentration on the optical characteristics of Cr3+:ZnGa2O4 transparent ceramics exhibiting persistent luminescence. Optical Materials, 2022, 125, 112127.	3.6	6

#	Article	IF	CITATIONS
37	Distribution, source apportionment and health risk assessment of phthalate esters in outdoor dust samples on Tibetan Plateau, China. Science of the Total Environment, 2022, 834, 155103.	8.0	10
38	Optimal control of the multi-module vibration-driven locomotion robot. Journal of Sound and Vibration, 2022, 527, 116867.	3.9	10
39	Atom-dispersed copper and nano-palladium in the boron-carbon-nitrogen matric cooperate to realize the efficient purification of nitrate wastewater and the electrochemical synthesis of ammonia. Journal of Hazardous Materials, 2022, 434, 128909.	12.4	21
40	Snake-worm: A Bi-modal Locomotion Robot. Journal of Bionic Engineering, 2022, 19, 1272-1287.	5.0	12
41	Identification of High δ <sup>18</sup> O Adakiteâ€Like Granites in SE Tibet: Implication for Diapiric Relamination of Subducted Sediments. Geophysical Research Letters, 2022, 49, .	4.0	3
42	Spatial distribution, receptor modelling and risk assessment of organophosphate esters in surface water from the largest freshwater lake in China. Ecotoxicology and Environmental Safety, 2022, 238, 113618.	6.0	6
43	Persulfate-based advanced oxidation processes: The new hope brought by nanocatalyst immobilization. , 2022, 1, 67-91.		13
44	CleanSeq: A Pipeline for Contamination Detection, Cleanup, and Mutation Verifications from Microbial Genome Sequencing Data. Applied Sciences (Switzerland), 2022, 12, 6209.	2.5	3
45	Photoinducible Azobenzene trimethylammonium bromide (AzoTAB)-mediated giant vesicle fusion compatible with synthetic protein translation reactions. Biochemical and Biophysical Research Communications, 2022, 618, 113-118.	2.1	4
46	Steady-state dynamics and discontinuity-induced sliding bifurcation of a multi-module piecewise-smooth vibration-driven system with dry friction. Communications in Nonlinear Science and Numerical Simulation, 2022, 114, 106704.	3.3	5
47	Time-Delayed Feedback Control Design and Its Application for Vibration Absorption. IEEE Transactions on Industrial Electronics, 2021, 68, 8593-8602.	7.9	16
48	Government subsidies, R&D investment and innovation performance: analysis from pharmaceutical sector in China. Technology Analysis and Strategic Management, 2021, 33, 535-553.	3.5	98
49	Influence of freeze-thaw cycles on microstructure and hydraulic conductivity of saline intact loess. Cold Regions Science and Technology, 2021, 181, 103183.	3.5	62
50	Development of White Persistent Phosphors by Manipulating Lanthanide Ions in Gadolinium Gallium Garnets. Advanced Photonics Research, 2021, 2, 2000102.	3.6	10
51	Structural insight into a CH1 β-glucosidase from the oleaginous microalga, Nannochloropsis oceanica. International Journal of Biological Macromolecules, 2021, 170, 196-206.	7.5	10
52	Mono-2-ethylhexyl phthalate drives progression of PINK1-parkin-mediated mitophagy via increasing mitochondrial ROS to exacerbate cytotoxicity. Redox Biology, 2021, 38, 101776.	9.0	56
53	The requirement of cellularity for abiogenesis. Computational and Structural Biotechnology Journal, 2021, 19, 2202-2212.	4.1	2
54	Zwitterionic liquid crystalline polythiophene as an antibiofouling biomaterial. Journal of Materials Chemistry B, 2021, 9, 349-356.	5.8	5

JIAN XU

#	Article	IF	CITATIONS
55	Bi-objective optimization for improving the locomotion performance of the vibration-driven robot. Archive of Applied Mechanics, 2021, 91, 2073-2088.	2.2	21
56	Meta-Apo improves accuracy of 16S-amplicon-based prediction of microbiome function. BMC Genomics, 2021, 22, 9.	2.8	15
57	D <sub>2</sub> O-Probed Raman Microspectroscopy Distinguishes the Metabolic Dynamics of Macromolecules in Organellar Anticancer Drug Response. Analytical Chemistry, 2021, 93, 2125-2134.	6.5	24
58	Spatial distribution, historical trend, and ecological risk assessment of phthalate esters in sediment from Taihu Lake, China. Environmental Science and Pollution Research, 2021, 28, 25207-25217.	5.3	13
59	Arginine methylation of R81 in Smad6 confines BMP-induced Smad1 signaling. Journal of Biological Chemistry, 2021, 296, 100496.	3.4	4
60	Enantioselective [4 + 2] Cycloaddition/Cyclization Cascade Reaction and Total Synthesis of <i>cis</i> -Bis(cyclotryptamine) Alkaloids. Organic Letters, 2021, 23, 1856-1861.	4.6	19
61	Distribution, source apportionment, and health risk assessment of phthalate esters in indoor dust samples across China. Environmental Sciences Europe, 2021, 33, .	5.5	32
62	Microbiome Search Engine 2: a Platform for Taxonomic and Functional Search of Global Microbiomes on the Whole-Microbiome Level. MSystems, 2021, 6, .	3.8	14
63	Corrosion Behavior of Rockbolts in Simulated Underground Mining Solutions Using Macro-scale and Micro-scale Electrochemical Measurements. Journal of Materials Engineering and Performance, 2021, 30, 2632-2644.	2.5	2
64	Intramolecular Stereoselective Stetter Reaction Catalyzed by Benzaldehyde Lyase. Angewandte Chemie - International Edition, 2021, 60, 9326-9329.	13.8	16
65	Intramolecular Stereoselective Stetter Reaction Catalyzed by Benzaldehyde Lyase. Angewandte Chemie, 2021, 133, 9412-9415.	2.0	5
66	Comparative Efficacy of the Novel Diarylquinoline TBAJ-587 and Bedaquiline against a Resistant <i>Rv0678</i> Mutant in a Mouse Model of Tuberculosis. Antimicrobial Agents and Chemotherapy, 2021, 65, .	3.2	26
67	Permeability and Microstructure of a Saline Intact Loess after Dry-Wet Cycles. Advances in Civil Engineering, 2021, 2021, 1-18.	0.7	8
68	Evolution of Ycf54-independent chlorophyll biosynthesis in cyanobacteria. Proceedings of the National Academy of Sciences of the United States of America, 2021, 118, .	7.1	7
69	Giant Vesicles Produced with Phosphatidylcholines (PCs) and Phosphatidylethanolamines (PEs) by Water-in-Oil Inverted Emulsions. Life, 2021, 11, 223.	2.4	5
70	Dissolution Behaviour of Laves Phase in P92 High Alloy Steel in Alkaline Solutions. Journal of the Electrochemical Society, 2021, 168, 031505.	2.9	3
71	Simultaneous enantioselective analysis of illicit drugs in wastewater and surface water by chiral LC–MS/MS: A pilot study on a wastewater treatment plant and its receiving river. Environmental Pollution, 2021, 273, 116424.	7.5	18
72	Wearable Glucose Monitoring and Implantable Drug Delivery Systems for Diabetes Management. Advanced Healthcare Materials, 2021, 10, e2100194.	7.6	38

#	Article	IF	CITATIONS
73	Does Intellectual Capital Investment Improve Financial Competitiveness and Green Innovation Performance? Evidence from Renewable Energy Companies in China. Mathematical Problems in Engineering, 2021, 2021, 1-13.	1.1	14
74	Longitudinal Multi-omics and Microbiome Meta-analysis Identify an Asymptomatic Gingival State That Links Gingivitis, Periodontitis, and Aging. MBio, 2021, 12, .	4.1	24
75	Active Thermal Management of High-Power LED Through Chip on Thermoelectric Cooler. IEEE Transactions on Electron Devices, 2021, 68, 1753-1756.	3.0	18
76	Genome engineering of <i>Nannochloropsis</i> with hundredâ€kilobase fragment deletions by Cas9 cleavages. Plant Journal, 2021, 106, 1148-1162.	5.7	19
77	Experimental study of event-based neural network control on parallel manipulator. Mechatronics, 2021, 75, 102514.	3.3	6
78	Do Intellectual Capital Elements Spur Firm Performance? Evidence from the Textile and Apparel Industry in China. Mathematical Problems in Engineering, 2021, 2021, 1-12.	1.1	13
79	One-Cell Metabolic Phenotyping and Sequencing of Soil Microbiome by Raman-Activated Gravity-Driven Encapsulation (RAGE). MSystems, 2021, 6, e0018121.	3.8	21
80	Image-based prediction of granular flow behaviors in a wedge-shaped hopper by combing DEM and deep learning methods. Powder Technology, 2021, 383, 159-166.	4.2	16
81	Unraveling the Luminescence Quenching of Phosphors under High-Power-Density Excitation. Acta Materialia, 2021, 209, 116813.	7.9	31
82	Enantioselective Synthesis of 3‧ubstituted 3â€Aminoâ€2â€oxindoles by Amination with Anilines. Chemistry - A European Journal, 2021, 27, 9272-9275.	3.3	13
83	Near-infrared Phosphors: Photophysical Properties of Calcium-doped YSGG:Cr4+. Sensors and Materials, 2021, 33, 2227.	0.5	3
84	Culture-Free Identification and Metabolic Profiling of Microalgal Single Cells via Ensemble Learning of Ramanomes. Analytical Chemistry, 2021, 93, 8872-8880.	6.5	16
85	A Visualization Method of Quantifying Carbon Combustion Energy in the Sintering Packed Bed. ISIJ International, 2021, 61, 1801-1807.	1.4	2
86	Quest for a pristine unreconstructed <mml:math xmlns:mml="http://www.w3.org/1998/Math/MathML"&gt; <mml:mrow> <mml:msub> <mml:mi> SrTiO </mml:mi> <mm surface: An atomically resolved study via noncontact atomic force microscopy. Physical Review B, 2021, 103, .</mm </mml:msub></mml:mrow></mml:math 	l:mn>3 </td <td>mml:mn&gt;14</td>	mml:mn>14
87	Study on Strength Behavior of Basalt Fiber-Reinforced Loess by Digital Image Technology (DIT) and Scanning Electron Microscope (SEM). Arabian Journal for Science and Engineering, 2021, 46, 11319-11338.	3.0	43
88	Active Human and Murine Tumor Necrosis Factor α Cytokines Produced from Silkworm Baculovirus Expression System. Insects, 2021, 12, 517.	2.2	3
89	Identification of antigenic domains and peptides from VP15 of white spot syndrome virus and their antiviral effects in Marsupenaeus japonicus. Scientific Reports, 2021, 11, 12766.	3.3	8
90	Triaxial Shear Behavior of Basalt Fiber-Reinforced Loess Based on Digital Image Technology. KSCE Journal of Civil Engineering, 2021, 25, 3714-3726.	1.9	37

#	Article	IF	CITATIONS
91	Multimodal vibration suppression of nonlinear Euler–Bernoulli beam by multiple time-delayed vibration absorbers. Meccanica, 2021, 56, 2429-2449.	2.0	4
92	Manipulating fatty-acid profile at unit chain-length resolution in the model industrial oleaginous microalgae Nannochloropsis. Metabolic Engineering, 2021, 66, 157-166.	7.0	14
93	Utilization and impacts of hydrogen in the ironmaking processes: A review from lab-scale basics to industrial practices. International Journal of Hydrogen Energy, 2021, 46, 26646-26664.	7.1	46
94	Integrated Addressable Dynamic Droplet Array (aDDA) as Subâ€Nanoliter Reactors for Highâ€Coverage Genome Sequencing of Single Yeast Cells. Small, 2021, 17, 2100325.	10.0	4
95	Asymmetric Catalytic Concise Synthesis of Hetero-3,3′-Bisoxindoles for the Construction of Bispyrroloindoline Alkaloids. CCS Chemistry, 2021, 3, 1894-1902.	7.8	30
96	Occurrence, sources, and ecological risks of three classes of insecticides in sediments of the Liaohe River basin, China. Environmental Science and Pollution Research, 2021, 28, 62726-62735.	5.3	19
97	A novel origami mechanical metamaterial based on Miura-variant designs: exceptional multistability and shape reconfigurability. Smart Materials and Structures, 2021, 30, 085029.	3.5	17
98	Fate of antibiotic resistance genes in farmland soil applied with three different fertilizers during the growth cycle of pakchoi and after harvesting. Journal of Environmental Management, 2021, 289, 112576.	7.8	16
99	Exploring the Nonlinear Effect of Intellectual Capital on Financial Performance: Evidence from Listed Shipping Companies in China. Complexity, 2021, 2021, 1-12.	1.6	9
100	A Scale-Free, Fully Connected Global Transition Network Underlies Known Microbiome Diversity. MSystems, 2021, 6, e0039421.	3.8	5
101	Production of an active Mus musculus IL-3 using updated silkworm-based baculovirus expression vector system. Journal of Asia-Pacific Entomology, 2021, 24, 544-549.	0.9	0
102	BaTiF <sub>6</sub> :Mn <sup>4+</sup> Red Phosphor: Synthesis of Single Crystals at Room Temperature and the High Hydrolysis-Resistant Property. Inorganic Chemistry, 2021, 60, 13212-13221.	4.0	7
103	Variability in Indonesian Throughflow Upper Hydrology in Response to Precessionâ€Induced Tropical Climate Processes Over the Past 120Âkyr. Journal of Geophysical Research: Oceans, 2021, 126, e2020JC017014.	2.6	4
104	Intra-Ramanome Correlation Analysis Unveils Metabolite Conversion Network from an Isogenic Population of Cells. MBio, 2021, 12, e0147021.	4.1	8
105	Does Intellectual Capital Measurement Matter in Financial Performance? An Investigation of Chinese Agricultural Listed Companies. Agronomy, 2021, 11, 1872.	3.0	15
106	pH-responsive pickering foam created from self-aggregate polymer using dynamic covalent bond. Journal of Colloid and Interface Science, 2021, 597, 383-392.	9.4	12
107	Occurrence, bioaccumulation and toxicological effect of drugs of abuse in aquatic ecosystem: A review. Environmental Research, 2021, 200, 111362.	7.5	22
108	Modeling of coupled transfer of water, heat and solute in saline loess considering sodium sulfate crystallization. Cold Regions Science and Technology, 2021, 189, 103335.	3.5	81

#	Article	IF	CITATIONS
109	Low-Temperature Hydrogenation of Toluene Using an Iron-Promoted Molybdenum Carbide Catalyst. Catalysts, 2021, 11, 1079.	3.5	2
110	Fabrication of single-mode circular optofluidic waveguides in fused silica using femtosecond laser microfabrication. Optics and Laser Technology, 2021, 141, 107118.	4.6	20
111	A milliliter to picoliter-level centrifugal microfluidic concentrator for fast pathogen detection and antimicrobial susceptibility testing. Sensors and Actuators B: Chemical, 2021, 343, 130117.	7.8	3
112	Tissue-specific accumulation, elimination, and toxicokinetics of illicit drugs in adult zebrafish (Danio) Tj ETQq0 0 (	D rgBT /Ov	erlock 10 Tf

113	Laser multifunctional fabrication of metallic microthermal components embedded in fused silica for microfluidic applications. Optics and Laser Technology, 2021, 144, 107413.	4.6	6
114	Does intellectual capital investment enhance firm performance? Evidence from pharmaceutical sector in China. Technology Analysis and Strategic Management, 2021, 33, 1006-1021.	3.5	22
115	Model-Free Control of Flexible Manipulator Based on Intrinsic Design. IEEE/ASME Transactions on Mechatronics, 2021, 26, 2641-2652.	5.8	9
116	Cement-Improved Wetting Resistance of Coarse Saline Soils in Northwest China. Journal of Testing and Evaluation, 2021, 49, 20180533.	0.7	3
117	Cyan-Emitting Sialon-Polytypoid Phosphor Discovered by a Single-Particle-Diagnosis Approach. ECS Journal of Solid State Science and Technology, 2021, 10, 116002.	1.8	2
118	How Many Electron Traps are formed in Persistent Phosphors?. ECS Journal of Solid State Science and Technology, 2021, 10, 116003.	1.8	8
119	Time-Delay-Based Direct Wave Control of the Phononic Beam. , 2021, , 193-199.		0
120	Design of a <b> <i>β</i> </b> -SiAlON:Eu based phosphor-in-glass film with high saturation threshold for high-luminance laser-driven backlighting. Applied Physics Letters, 2021, 119, .	3.3	5
121	High-Pressure Photoluminescence Properties of Cr <sup>3+</sup> -Doped LaGaO <sub>3</sub> Perovskites Modulated by Pressure-Induced Phase Transition. Inorganic Chemistry, 2021, 60, 19253-19262.	4.0	12
122	Event-Triggered Adaptive Neural Network Control of Manipulators with Model-Based Weights Initialization Method. International Journal of Precision Engineering and Manufacturing - Green Technology, 2020, 7, 443-454.	4.9	7
123	An analytical method for studying double Hopf bifurcations induced by two delays in nonlinear differential systems. Science China Technological Sciences, 2020, 63, 597-602.	4.0	9
124	Subduction polarity of the Ailaoshan Ocean (eastern Paleotethys): Constraints from detrital zircon U-Pb and Hf-O isotopes for the Longtan Formation. Bulletin of the Geological Society of America, 2020, 132, 987-996.	3.3	23
124 125	Subduction polarity of the Ailaoshan Ocean (eastern Paleotethys): Constraints from detrital zircon U-Pb and Hf-O isotopes for the Longtan Formation. Bulletin of the Geological Society of America,	3.3 4.7	23 42

#	Article	IF	CITATIONS
127	Skin benefits of moisturising body wash formulas for children with atopic dermatitis: A randomised controlled clinical study in China. Australasian Journal of Dermatology, 2020, 61, e54-e59.	0.7	18
128	A systematic and methodical approach for the efficient purification of recombinant protein from silkworm larval hemolymph. Journal of Chromatography B: Analytical Technologies in the Biomedical and Life Sciences, 2020, 1138, 121964.	2.3	5
129	Identification of secretion domain of Neospora caninum profilin. Biochemical and Biophysical Research Communications, 2020, 522, 8-13.	2.1	0
130	Recent massive incidents for subway construction in soft alluvial deposits of Taiwan: A review. Tunnelling and Underground Space Technology, 2020, 96, 103178.	6.2	67
131	Influence of particle packed pattern on the transient granular flow in a wedge-shaped hopper. Advanced Powder Technology, 2020, 31, 670-677.	4.1	7
132	<i>Dynamic Meta-Storms</i> enables comprehensive taxonomic and phylogenetic comparison of shotgun metagenomes at the species level. Bioinformatics, 2020, 36, 2308-2310.	4.1	12
133	Effect of freeze-thaw on freezing point of a saline loess. Cold Regions Science and Technology, 2020, 170, 102922.	3.5	33
134	Dynamic liquid phase deposition of doped nanostructured PANI tube sensor for trace-level NH3 gas detection. Sensors and Actuators B: Chemical, 2020, 305, 127459.	7.8	9
135	First Continuous Measurement of Gaseous and Particulate Formic Acid in a Suburban Area of East China: Seasonality and Gas–Particle Partitioning. ACS Earth and Space Chemistry, 2020, 4, 157-167.	2.7	18
136	Transient Dynamics of a Miura-Origami Tube during Free Deployment. Physical Review Applied, 2020, 14, .	3.8	15
137	Confined-Melting-Assisted Synthesis of Bismuth Silicate Glass-Ceramic Nanoparticles: Formation and Optical Thermometry Investigation. ACS Applied Materials & Interfaces, 2020, 12, 55195-55204.	8.0	35
138	Microsized Red Luminescent MgAl <sub>2</sub> O <sub>4</sub> :Mn <sup>4+</sup> Single-Crystal Phosphor Grown in Molten Salt for White LEDs. Inorganic Chemistry, 2020, 59, 18374-18383.	4.0	19
139	Positive dielectrophoresis–based Raman-activated droplet sorting for culture-free and label-free screening of enzyme function in vivo. Science Advances, 2020, 6, eabb3521.	10.3	48
140	Printable Nonenzymatic Glucose Biosensors Using Carbon Nanotube-PtNP Nanocomposites Modified with AuRu for Improved Selectivity. ACS Biomaterials Science and Engineering, 2020, 6, 5315-5325.	5.2	27
141	Preparation of divalent antigen-displaying enveloped virus-like particles using a single recombinant Bombyx mori nucleopolyhedrovirus bacmid in silkworms. Journal of Biotechnology, 2020, 323, 92-97.	3.8	2
142	Damage of saline intact loess after dry-wet and its interpretation based on SEM and NMR. Soils and Foundations, 2020, 60, 911-928.	3.1	54
143	Anti-Biofouling Strategies for Long-Term Continuous Use of Implantable Biosensors. Chemosensors, 2020, 8, 66.	3.6	56
144	Spontaneous droplet generation <i>via</i> surface wetting. Lab on A Chip, 2020, 20, 3544-3551.	6.0	5

#	Article	IF	CITATIONS
145	Ni-modified magnetic nanoparticles for affinity purification of His-tagged proteins from the complex matrix of the silkworm fat body. Journal of Nanobiotechnology, 2020, 18, 159.	9.1	15
146	The NanDeSyn database for <i>Nannochloropsis</i> systems and synthetic biology. Plant Journal, 2020, 104, 1736-1745.	5.7	37
147	Degradation of Ketamine and Methamphetamine by the UV/H2O2 System: Kinetics, Mechanisms and Comparison. Water (Switzerland), 2020, 12, 2999.	2.7	5
148	Hexagonal Sr <sub>1â^x/2</sub> Al <sub>2â^x</sub> Si <sub>x</sub> O <sub>4</sub> :Eu <sup>2+</sup> ,Dy <sup>3+ceramics with tuneable persistent luminescence properties. Dalton Transactions, 2020, 49, 16849-16859.</sup>	>tra <b>ns</b> pare	nt 13
149	Energy determines multiple stability in time-delayed systems. Nonlinear Dynamics, 2020, 102, 2399-2416.	5.2	8
150	Rational Optimization of Raman-Activated Cell Ejection and Sequencing for Bacteria. Analytical Chemistry, 2020, 92, 8081-8089.	6.5	10
151	The Role of Corporate Political Connections in Commercial Lawsuits: Evidence From Chinese Courts. Comparative Political Studies, 2020, 53, 2321-2358.	3.6	16
152	Indoâ€Pacific Hydroclimate in Response to Changes of the Intertropical Convergence Zone: Discrepancy on Precession and Obliquity Bands Over the Last 410Âkyr. Journal of Geophysical Research D: Atmospheres, 2020, 125, e2019JD032125.	3.3	9
153	In-plane gait planning for earthworm-like metameric robots using genetic algorithm. Bioinspiration and Biomimetics, 2020, 15, 056012.	2.9	9
154	Modeling of wetting deformation of coarse saline soil with an improved von Wolffersdorff model. Bulletin of Engineering Geology and the Environment, 2020, 79, 4783-4804.	3.5	4
155	From asymmetrical to balanced genomic diversification during rediploidization: Subgenomic evolution in allotetraploid fish. Science Advances, 2020, 6, eaaz7677.	10.3	59
156	Numerical Analysis of Effects of Different Blast Parameters on the Gas and Burden Distribution Characteristics Inside Blast Furnace. ISIJ International, 2020, 60, 856-864.	1.4	5
157	Aqueous chlorination of ephedrine: Kinetic, reaction mechanism and toxicity assessment. Science of the Total Environment, 2020, 740, 140146.	8.0	10
158	Phenome–Genome Profiling of Single Bacterial Cell by Ramanâ€Activated Gravityâ€Driven Encapsulation and Sequencing. Small, 2020, 16, e2001172.	10.0	33
159	Transient shrinkage behavior of wustite-centered binary/ternary/quaternary/quinary-component oxide packed beds in a reducing atmosphere up to 1773ÂK. Ceramics International, 2020, 46, 11854-11860.	4.8	3
160	Effective Ratiometric Luminescent Thermal Sensor by Cr <sup>3+</sup> â€Doped Mullite Bi <sub>2</sub> Al <sub>4</sub> O <sub>9</sub> with Robust and Reliable Performances. Advanced Optical Materials, 2020, 8, 2000124.	7.3	114
161	Analytical solutions for steady state responses of an infinite Euler-Bernoulli beam on a nonlinear viscoelastic foundation subjected to a harmonic moving load. Journal of Sound and Vibration, 2020, 476, 115271.	3.9	15
162	Efficient and Low-Cost Error Removal in DNA Synthesis by a High-Durability MutS. ACS Synthetic Biology, 2020, 9, 940-952.	3.8	4

JIAN XU

#	Article	IF	CITATIONS
163	Building a PubMed knowledge graph. Scientific Data, 2020, 7, 205.	5.3	94
164	Industry-friendly synthesis and high saturation threshold of a LuAG:Ce/glass composite film realizing high-brightness laser lighting. Journal of the European Ceramic Society, 2020, 40, 6031-6036.	5.7	30
165	Adaptive evolution of low-salinity tolerance and hypoosmotic regulation in a euryhaline teleost, Takifugu obscurus. Marine Biology, 2020, 167, 1.	1.5	16
166	Effect of freeze-thaw on freezing point and thermal conductivity of loess. Arabian Journal of Geosciences, 2020, 13, 1.	1.3	14
167	Remnants of a Middle Triassic island arc on western margin of South China Block: Evidence for bipolar subduction of the Paleotethyan Ailaoshan Ocean. Lithos, 2020, 360-361, 105447.	1.4	17
168	Theoretical Parameter-Free Analysis Model for Temperature-Programmed Desorption (TPD) Spectra. ACS Omega, 2020, 5, 4148-4157.	3.5	7
169	Worm-like motion enabled by changing the position of mass center in the anisotropic environment. Archive of Applied Mechanics, 2020, 90, 1059-1071.	2.2	2
170	The generalization of equal-peak method for delay-coupled nonlinear system. Physica D: Nonlinear Phenomena, 2020, 403, 132340.	2.8	18
171	Chemical removal and selectivity reduction of nitrate from water by (nano) zero-valent iron/activated carbon micro-electrolysis. Chemosphere, 2020, 248, 125986.	8.2	52
172	A novel Z-scheme AgBr/P-g-C3N4 heterojunction photocatalyst: Excellent photocatalytic performance and photocatalytic mechanism for ephedrine degradation. Applied Catalysis B: Environmental, 2020, 266, 118614.	20.2	183
173	Freeform Microfluidic Networks Encapsulated in Laserâ€Printed 3D Macroscale Glass Objects. Advanced Materials Technologies, 2020, 5, 1900989.	5.8	29
174	Multiple-Disease Detection and Classification across Cohorts via Microbiome Search. MSystems, 2020, 5, .	3.8	16
175	High dielectric performance of (Nb5+, Lu3+) co-doped TiO2 ceramics in a broad temperature range. Materials Letters, 2020, 271, 127838.	2.6	19
176	Transcriptomic and proteomic choreography in response to light quality variation reveals key adaption mechanisms in marine Nannochloropsis oceanica. Science of the Total Environment, 2020, 720, 137667.	8.0	20
177	Design of a CaAlSiN3:Eu/glass composite film: Facile synthesis, high saturation-threshold and application in high-power laser lighting. Journal of the European Ceramic Society, 2020, 40, 4704-4708.	5.7	33
178	One-Step Large-Scale Nanotexturing of Nonplanar PTFE Surfaces to Induce Bactericidal and Anti-inflammatory Properties. ACS Applied Materials & Interfaces, 2020, 12, 26893-26904.	8.0	14
179	Zwitterionic Porous Conjugated Polymers as a Versatile Platform for Antibiofouling Implantable Bioelectronics. ACS Applied Polymer Materials, 2020, 2, 528-536.	4.4	17
180	Mechanistic Understanding of the Dissolution Behavior of the Precipitates in 12Cr Martensitic Steel during Potentiodynamic Polarization in Strong Alkaline Solutions. Journal of the Electrochemical Society, 2020, 167, 141501.	2.9	4

#	Article	IF	CITATIONS
181	Occurrence and removal of illicit drugs in different wastewater treatment plants with different treatment techniques. Environmental Sciences Europe, 2020, 32, .	5.5	30
182	Antibiotic resistance genes in different animal manures and their derived organic fertilizer. Environmental Sciences Europe, 2020, 32, .	5.5	33
183	Impact of Environmental Investment on Financial Performance: Evidence from Chinese listed Companies. Polish Journal of Environmental Studies, 2020, 29, 2235-2245.	1.2	13
184	NEXUS BETWEEN INTELLECTUAL CAPITAL AND FINANCIAL PERFORMANCE: AN INVESTIGATION OF CHINESE MANUFACTURING INDUSTRY. Journal of Business Economics and Management, 2020, 22, 217-235.	2.4	28
185	Importance of gas-particle partitioning of ammonia in haze formation in the rural agricultural environment. Atmospheric Chemistry and Physics, 2020, 20, 7259-7269.	4.9	31
186	The Impact of Intellectual Capital on Firm Performance: A Modified and Extended VAIC Model. Journal of Competitiveness, 2020, 12, 161-176.	3.0	73
187	Assessing contributions of natural surface and anthropogenic emissions to atmospheric mercury in a fast-developing region of eastern China from 2015 to 2018. Atmospheric Chemistry and Physics, 2020, 20, 10985-10996.	4.9	5
188	Local coordination, electronic structure, and thermal quenching of Ce <sup>3+</sup> in isostructural Sr <sub>2</sub> GdAlO <sub>5</sub> and Sr <sub>3</sub> AlO <sub>4</sub> F phosphors. Journal of the American Ceramic Society, 2019, 102, 1316-1328.	3.8	10
189	Characteristics of particulate-bound mercury at typical sites situated on dust transport paths in China. Science of the Total Environment, 2019, 648, 1151-1160.	8.0	14
190	Reply to Sun et al., "Identifying Composition Novelty in Microbiome Studies: Improvement of Prediction Accuracy― MBio, 2019, 10, .	4.1	0
191	Denoising identification for nonlinear systems with distorted streaming. International Journal of Non-Linear Mechanics, 2019, 117, 103224.	2.6	3
192	Persistent energy transfer in ZGO:Cr <sup>3+</sup> ,Yb <sup>3+</sup> : a new strategy to design nano glass-ceramics featuring deep red and near infrared persistent luminescence. Physical Chemistry Chemical Physics, 2019, 21, 19458-19468.	2.8	34
193	Bend-Resistant Large Mode Area Fiber With an Azimuthally Segmented Trench in the Cladding. Journal of Lightwave Technology, 2019, 37, 3761-3769.	4.6	8
194	Genome assembly of Nannochloropsis oceanica provides evidence of host nucleus overthrow by the symbiont nucleus during speciation. Communications Biology, 2019, 2, 249.	4.4	29
195	Transformation of organic sulfur and its functional groups in nantong and laigang coal under microwave irradiation. Journal of Computational Chemistry, 2019, 40, 2749-2760.	3.3	15
196	R&D, Advertising and Firms' Financial Performance in South Korea: Does Firm Size Matter?. Sustainability, 2019, 11, 3764.	3.2	19
197	Downregulation of IncRNA AFAP1-AS1 by oridonin inhibits the epithelial-to-mesenchymal transition and proliferation of pancreatic cancer cells. Acta Biochimica Et Biophysica Sinica, 2019, 51, 814-825.	2.0	22
198	Analysis, design and experiment of continuous isolation structure with Local Quasi-Zero-Stiffness property by magnetic interaction. International Journal of Non-Linear Mechanics, 2019, 116, 289-301.	2.6	37

#	Article	IF	CITATIONS
199	Causes of Particle Trajectory Fluctuation on the Rotating Chute in Circumferential Direction at Bell-less Top with Parallel Type Hoppers. ISIJ International, 2019, 59, 1527-1533.	1.4	6
200	Patterns of Geographical and Potential Adaptive Divergence in the Genome of the Common Carp (Cyprinus carpio). Frontiers in Genetics, 2019, 10, 660.	2.3	12
201	Oridonin overcomes the gemcitabine resistant PANC-1/Gem cells by regulating GST pi and LRP/1 ERK/JNK signalling. OncoTargets and Therapy, 2019, Volume 12, 5751-5765.	2.0	29
202	Transcriptomic and proteomic responses to very low CO2 suggest multiple carbon concentrating mechanisms in Nannochloropsis oceanica. Biotechnology for Biofuels, 2019, 12, 168.	6.2	46
203	Preferential Tumor Accumulation of Polyglycerol Functionalized Nanodiamond Conjugated with Cyanine Dye Leading to Nearâ€Infrared Fluorescence In Vivo Tumor Imaging. Small, 2019, 15, e1901930.	10.0	37
204	Self-limited growth of an oxyhydroxide phase at the Fe3O4(001) surface in liquid and ambient pressure water. Journal of Chemical Physics, 2019, 151, 154702.	3.0	15
205	The allotetraploid origin and asymmetrical genome evolution of theÂcommon carp Cyprinus carpio. Nature Communications, 2019, 10, 4625.	12.8	156
206	Planar locomotion of earthworm-like metameric robots. International Journal of Robotics Research, 2019, 38, 1751-1774.	8.5	27
207	Prioritizing environmental risks of pharmaceuticals and personal care products in reclaimed water on urban green space in Beijing. Science of the Total Environment, 2019, 697, 133850.	8.0	23
208	Intellectual Capital, Technological Innovation and Firm Performance: Evidence from China's Manufacturing Sector. Sustainability, 2019, 11, 5328.	3.2	52
209	Analysis and experiment of time-delayed optimal control for vehicle suspension system. Journal of Sound and Vibration, 2019, 446, 144-158.	3.9	37
210	A Microbiome-Based Index for Assessing Skin Health and Treatment Effects for Atopic Dermatitis in Children. MSystems, 2019, 4, .	3.8	22
211	Kinetic and mechanistic study of sulfadimidine photodegradation under simulated sunlight irradiation. Environmental Sciences Europe, 2019, 31, .	5.5	13
212	Development of SpyTag/SpyCatcher-Bacmid Expression Vector System (SpyBEVS) for Protein Bioconjugations Inside of Silkworms. International Journal of Molecular Sciences, 2019, 20, 4228.	4.1	8
213	Characteristics and sources of aerosol aminiums over the eastern coast of China: insights from the integrated observations in a coastal city, adjacent island and surrounding marginal seas. Atmospheric Chemistry and Physics, 2019, 19, 10447-10467.	4.9	29
214	Ratiometric Luminescent Thermometers with a Customized Phase-Transition-Driven Fingerprint in Perovskite Oxides. ACS Applied Materials & Interfaces, 2019, 11, 38937-38945.	8.0	57
215	Neospora caninum antigens displaying virus-like particles as a bivalent vaccine candidate against neosporosis. Vaccine, 2019, 37, 6426-6434.	3.8	8
216	Biosynthesis of Triacylglycerol Molecules with a Tailored PUFA Profile in Industrial Microalgae. Molecular Plant, 2019, 12, 474-488.	8.3	73

#	Article	IF	CITATIONS
217	Effect of cross-section shape of rotating chute on particle movement and distribution at the throat of a bell-less top blast furnace. Particuology, 2019, 44, 194-206.	3.6	18
218	Parameter design for a vibration absorber with time-delayed feedback control. Acta Mechanica Sinica/Lixue Xuebao, 2019, 35, 624-640.	3.4	19
219	Development and application of the analytical method for illicit drugs and metabolites in fish tissues. Chemosphere, 2019, 233, 532-541.	8.2	20
220	Hydrogen impact on the shrinkage behaviors of wustite packed beds above 900°C. International Journal of Hydrogen Energy, 2019, 44, 19555-19562.	7.1	6
221	Expression and Purification of Vaccinia Virus DNA Topoisomerase IB Produced in the Silkworm–Baculovirus Expression System. Molecular Biotechnology, 2019, 61, 622-630.	2.4	6
222	Intellectual Capital Performance of the Textile Industry in Emerging Markets: A Comparison with China and South Korea. Sustainability, 2019, 11, 2354.	3.2	39
223	Protein expression analysis revealed a fine-tuned mechanism of in situ detoxification pathway for the tolerant industrial yeast Saccharomyces cerevisiae. Applied Microbiology and Biotechnology, 2019, 103, 5781-5796.	3.6	10
224	Nonlinear Piezoelectric Structure for Ultralow-frequency Band Vibration Energy Harvesting with Magnetic Interaction. International Journal of Precision Engineering and Manufacturing - Green Technology, 2019, 6, 671-679.	4.9	15
225	Ramanome technology platform for label-free screening and sorting of microbial cell factories at single-cell resolution. Biotechnology Advances, 2019, 37, 107388.	11.7	55
226	Removal of methamphetamine by UV-activated persulfate: Kinetics and mechanisms. Journal of Photochemistry and Photobiology A: Chemistry, 2019, 379, 32-38.	3.9	25
227	Occurrence, distribution and risk assessment of abused drugs and their metabolites in a typical urban river in north China. Frontiers of Environmental Science and Engineering, 2019, 13, 1.	6.0	21
228	Secretory Nanoparticles of Neospora caninum Profilin-Fused with the Transmembrane Domain of GP64 from Silkworm Hemolymph. Nanomaterials, 2019, 9, 593.	4.1	5
229	Uncovering the Origin of the Emitting States in Bi <sup>3+</sup> -Activated CaMO <sub>3</sub> (M = Zr,) Tj ETC Chemistry C, 2019, 123, 14677-14688.	Qq1 1 0.78 3.1	34314 rgBT 44
230	Polarization-insensitive space-selective etching in fused silica induced by picosecond laser irradiation. Applied Surface Science, 2019, 485, 188-193.	6.1	43
231	Shear strength and damage mechanism of saline intact loess after freeze-thaw cycling. Cold Regions Science and Technology, 2019, 164, 102779.	3.5	69
232	Parameter identification of time-delayed nonlinear systems: An integrated method with adaptive noise correction. Journal of the Franklin Institute, 2019, 356, 5858-5880.	3.4	13
233	Investigation of laser-induced luminescence saturation in a single-crystal YAC:Ce phosphor: Towards unique architecture, high saturation threshold, and high-brightness laser-driven white lighting. Journal of Luminescence, 2019, 212, 279-285.	3.1	71
234	Frost Heave of Irrigation Canals in Seasonal Frozen Regions. Advances in Civil Engineering, 2019, 2019, 1-14.	0.7	7

#	Article	IF	CITATIONS
235	Improving performance: recent progress on vibration-driven locomotion systems. Nonlinear Dynamics, 2019, 98, 2651-2669.	5.2	39
236	Carbon formation on the surface during the reduction of iron oxide particles by CO and CO/H2 mixtures. Chemical Engineering Science, 2019, 205, 238-247.	3.8	8
237	When Did the Paleotethys Ailaoshan Ocean Close: New Insights From Detrital Zircon Uâ€Pb age and Hf Isotopes. Tectonics, 2019, 38, 1798-1823.	2.8	51
238	Estimation and improvement of cutting safety. Nonlinear Dynamics, 2019, 98, 2975-2988.	5.2	12
239	Interdisciplinary scholarly communication: an exploratory study for the field of joint attention. Scientometrics, 2019, 119, 1597-1619.	3.0	4
240	Knockdown of carbonate anhydrase elevates Nannochloropsis productivity at high CO2 level. Metabolic Engineering, 2019, 54, 96-108.	7.0	55
241	Fabrication of graphite via electrochemical conversion of CO2 in a CaCl2 based molten salt at a relatively low temperature. RSC Advances, 2019, 9, 8585-8593.	3.6	11
242	First Identification of Late Permian Nbâ€Enriched Basalts in Ailaoshan Region (SW Yunnan, China): Contribution From Emeishan Plume to Subduction of Eastern Paleotethys. Geophysical Research Letters, 2019, 46, 2511-2523.	4.0	35
243	Phase-field method for growth of iron whiskers in the presence of CO gas convection. Journal of Iron and Steel Research International, 2019, 26, 829-837.	2.8	4
244	The competitive adsorption behavior of CO and H2 molecules on FeO surface in the reduction process. International Journal of Hydrogen Energy, 2019, 44, 6427-6436.	7.1	22
245	Expression and purification of biologically active human granulocyte-macrophage colony stimulating factor (hCM-CSF) using silkworm-baculovirus expression vector system. Protein Expression and Purification, 2019, 159, 69-74.	1.3	9
246	Shear Strength Behavior of Coarse-Grained Saline Soils after Freeze-Thaw. KSCE Journal of Civil Engineering, 2019, 23, 2437-2452.	1.9	32
247	Kinetic and mechanistic investigation on the decomposition of ketamine by UV-254â€ <sup>-</sup> nm activated persulfate. Chemical Engineering Journal, 2019, 370, 19-26.	12.7	50
248	Identification of piecewise linear dynamical systems using physically-interpretable neural-fuzzy networks: Methods and applications to origami structures. Neural Networks, 2019, 116, 74-87.	5.9	18
249	Nanocomposites of Ag <sub>3</sub> PO <sub>4</sub> and Phosphorus-Doped Graphitic Carbon Nitride for Ketamine Removal. ACS Applied Nano Materials, 2019, 2, 2817-2829.	5.0	29
250	Modelling of regenerative and frictional cutting dynamics. International Journal of Mechanical Sciences, 2019, 156, 86-93.	6.7	31
251	Expression of the thermostable Moloney murine leukemia virus reverse transcriptase by silkworm-baculovirus expression system. Journal of Asia-Pacific Entomology, 2019, 22, 453-457.	0.9	7
252	Adsorption-enhanced oxidative desulfurization by a task-specific pyridinium-based porous ionic polymer. Fuel. 2019. 244. 439-446.	6.4	24

#	Article	IF	CITATIONS
253	Proteomic study uncovers molecular principles of single-cell-level phenotypic heterogeneity in lipid storage of Nannochloropsis oceanica. Biotechnology for Biofuels, 2019, 12, 21.	6.2	14
254	Expression, purification, and characterization of highly active endo-α-N-acetylgalactosaminidases expressed by silkworm-baculovirus expression system. Journal of Asia-Pacific Entomology, 2019, 22, 404-408.	0.9	5
255	Openness and Security in Cloud Computing Services: Assessment Methods and Investment Strategies Analysis. IEEE Access, 2019, 7, 29038-29050.	4.2	5
256	Design and experiment of nonlinear absorber for equal-peak and de-nonlinearity. Journal of Sound and Vibration, 2019, 449, 274-299.	3.9	26
257	The impact of intellectual capital on SMEs' performance in China. Journal of Intellectual Capital, 2019, 20, 488-509.	5.4	110
258	Biomimetic Accumulation of Methamphetamine and Its Metabolite Amphetamine by Diffusive Gradients in Thin Films to Estimate Their Bioavailability in Zebrafish. Environmental Science and Technology Letters, 2019, 6, 708-713.	8.7	15
259	A Drive to Driven Model of Mapping Intraspecific Interaction Networks. IScience, 2019, 22, 109-122.	4.1	11
260	Evaporation-Induced Water and Solute Coupled Transport in Saline Loess Columns in Closed and Open Systems. Geofluids, 2019, 2019, 1-26.	0.7	0
261	Rethinking the Water Leak Incident of Tunnel LUO09 to Prepare for a Challenging Future. Advances in Civil Engineering, 2019, 2019, 1-11.	0.7	6
262	Using Post-Harvest Waste to Improve Shearing Behaviour of Loess and Its Validation by Multiscale Direct Shear Tests. Applied Sciences (Switzerland), 2019, 9, 5206.	2.5	16
263	Carbon-free synthesis and luminescence saturation in a thick YAC:Ce film for laser-driven white lighting. Journal of the European Ceramic Society, 2019, 39, 631-634.	5.7	24
264	High-throughput multi-resolution three dimensional laser printing. Physica Scripta, 2019, 94, 015501.	2.5	11
265	Suppression of oscillatory congestion via trunk link bandwidth and control gain in star network. Applied Mathematics and Mechanics (English Edition), 2019, 40, 25-48.	3.6	2
266	Dynamics and Realization of a Feedback-Controlled Nonlinear Isolator With Variable Time Delay. Journal of Vibration and Acoustics, Transactions of the ASME, 2019, 141, .	1.6	20
267	Changes of provenance of Permian and Triassic sedimentary rocks from the Ailaoshan suture zone (SW China) with implications for the closure of the eastern Paleotethys. Journal of Asian Earth Sciences, 2019, 170, 234-248.	2.3	24
268	Hydraulic conductivity of geosynthetic clay liners to inorganic waste leachate. Applied Clay Science, 2019, 168, 244-248.	5.2	28
269	A stretchable and bendable all-solid-state pseudocapacitor with dodecylbenzenesulfonate-doped polypyrrole-coated vertically aligned carbon nanotubes partially embedded in PDMS. Nanotechnology, 2019, 30, 095401.	2.6	16
270	Effects of Blast Furnace Main Trough Geometry on the Slagâ€Metal Separation Based on Numerical Simulation. Steel Research International, 2019, 90, 1800383.	1.8	6

#	Article	IF	CITATIONS
271	In-situ fabrication of Ag/P-g-C3N4 composites with enhanced photocatalytic activity for sulfamethoxazole degradation. Journal of Hazardous Materials, 2019, 366, 219-228.	12.4	104
272	DEM study on ternary-sized particle segregation during the sinter burden charging process. Powder Technology, 2019, 343, 422-435.	4.2	14
273	Persistent luminescence instead of phosphorescence: History, mechanism, and perspective. Journal of Luminescence, 2019, 205, 581-620.	3.1	425
274	Partitioning behavior, source identification, and risk assessment of perfluorinated compounds in an industry-influenced river. Environmental Sciences Europe, 2019, 31, .	5.5	16
275	Reconfigurable directional coupler in lithium niobate crystal fabricated by three-dimensional femtosecond laser focal field engineering. Photonics Research, 2019, 7, 503.	7.0	25
276	Mixed-coexistence of periodic orbits and chaotic attractors in an inertial neural system with a nonmonotonic activation function. Mathematical Biosciences and Engineering, 2019, 16, 6406-6425.	1.9	12
277	1.5μ4m persistent luminescence of Er3+ in Gd3Al5-xGaxO12 (GAGC) garnets via persistent energy transfer. , 2019, , .		2
278	Centimeterâ€Height 3D Printing with Femtosecond Laser Twoâ€Photon Polymerization. Advanced Materials Technologies, 2018, 3, 1700396.	5.8	64
279	An Extended Synchronization Method to Identify Slowly Time-Varying Parameters in Nonlinear Systems. IEEE Transactions on Signal Processing, 2018, 66, 438-448.	5.3	7
280	Quantitative comparison of binary particle mass and size segregation between serial and parallel type hoppers of blast furnace bell-less top charging system. Powder Technology, 2018, 328, 245-255.	4.2	26
281	Effects of bottom base shapes on burden profiles and burden size distributions in the upper part of a COREX shaft furnace based on DEM. Advanced Powder Technology, 2018, 29, 1014-1024.	4.1	24
282	Surface roughness: A review of its measurement at micro-/nano-scale. ChemistrySelect, 2018, 3, .	1.5	17
283	Model of a Frame of Dynamic Routing and Its Equilibrium. International Journal of Bifurcation and Chaos in Applied Sciences and Engineering, 2018, 28, 1850005.	1.7	0
284	Aerosol Brown Carbon from Dark Reactions of Syringol in Aqueous Aerosol Mimics. ACS Earth and Space Chemistry, 2018, 2, 608-617.	2.7	24
285	Toward Rechargeable Persistent Luminescence for the First and Third Biological Windows via Persistent Energy Transfer and Electron Trap Redistribution. Inorganic Chemistry, 2018, 57, 5194-5203.	4.0	100
286	Locomotion of two vibration-driven modules connected by a mechanical position limiter. International Journal of Mechanical Sciences, 2018, 137, 252-262.	6.7	7
287	Parameter design of a multi-delayed isolator with asymmetrical nonlinearity. International Journal of Mechanical Sciences, 2018, 138-139, 398-408.	6.7	28
288	A Galerkin discretisation-based identification for parameters in nonlinear mechanical systems. International Journal of Systems Science, 2018, 49, 908-919.	5.5	0

#	Article	IF	CITATIONS
289	Stability and Hopf bifurcation on four-neuron neural networks with inertia and multiple delays. Neurocomputing, 2018, 287, 34-44.	5.9	35
290	Optimized methods of chromatin immunoprecipitation for profiling histone modifications in industrial microalgae <i>Nannochloropsis</i> spp Journal of Phycology, 2018, 54, 358-367.	2.3	14
291	Microporous Luminescent Metal–Organic Framework for a Sensitive and Selective Fluorescence Sensing of Toxic Mycotoxin in Moldy Sugarcane. ACS Applied Materials & Interfaces, 2018, 10, 5618-5625.	8.0	121
292	Experiments on vibration-driven stick-slip locomotion: A sliding bifurcation perspective. Mechanical Systems and Signal Processing, 2018, 105, 261-275.	8.0	32
293	Prmt1 regulates craniofacial bone formation upstream of Msx1. Mechanisms of Development, 2018, 152, 13-20.	1.7	9
294	Production of a biologically active human basic fibroblast growth factor using silkworm-baculovirus expression vector system. Journal of Asia-Pacific Entomology, 2018, 21, 716-720.	0.9	2
295	Environmentally dependent dust chemistry of a super Asian dust storm in March 2010: observation and simulation. Atmospheric Chemistry and Physics, 2018, 18, 3505-3521.	4.9	24
296	Predicting trace metal bioavailability to chironomids in sediments by diffusive gradients in thin films. Science of the Total Environment, 2018, 636, 134-141.	8.0	23
297	Smartphone-based rapid quantification of viable bacteria by single-cell microdroplet turbidity imaging. Analyst, The, 2018, 143, 3309-3316.	3.5	29
298	Governing China's Coal Challenge: Changing Public Policy, Debate and Advocacy. Environmental Communication, 2018, 12, 575-588.	2.5	4
299	A parameter identification method for continuous-time nonlinear systems and its realization on a Miura-origami structure. Mechanical Systems and Signal Processing, 2018, 108, 369-386.	8.0	11
300	A novel energy harvesting device for ultralow frequency excitation. Energy, 2018, 151, 250-260.	8.8	18
301	A frequency-domain method for solving linear time delay systems with constant coefficients. Acta Mechanica Sinica/Lixue Xuebao, 2018, 34, 781-791.	3.4	1
302	Modelling and tuning for a time-delayed vibration absorber with friction. Journal of Sound and Vibration, 2018, 424, 137-157.	3.9	25
303	Bifurcation Analysis and Spatiotemporal Patterns in Unidirectionally Delay-Coupled Vibratory Gyroscopes. International Journal of Bifurcation and Chaos in Applied Sciences and Engineering, 2018, 28, 1850029.	1.7	2
304	Strength behaviors and meso-structural characters of loess after freeze-thaw. Cold Regions Science and Technology, 2018, 148, 104-120.	3.5	84
305	Synthesis of a novel one-dimensional BiOBr–Bi <sub>4</sub> O <sub>5</sub> Br <sub>2</sub> heterostructure with a high quality interface and its enhanced visible-light photocatalytic activity. CrystEngComm, 2018, 20, 2292-2298.	2.6	33
306	Heat transfer and water migration in loess slopes during freeze–thaw cycling in Northern Shaanxi, China. International Journal of Civil Engineering, 2018, 16, 1591-1605.	2.0	14

#	Article	IF	CITATIONS
307	Insights into the characteristics and sources of primary and secondary organic carbon: High time resolution observation in urban Shanghai. Environmental Pollution, 2018, 233, 1177-1187.	7.5	35
308	A new method to quantify the health risks from sources of perfluoroalkyl substances, combined with positive matrix factorization and risk assessment models. Environmental Toxicology and Chemistry, 2018, 37, 107-115.	4.3	7
309	Understanding success through the diversity of collaborators and the milestone of career. Journal of the Association for Information Science and Technology, 2018, 69, 87-97.	2.9	25
310	Dynamical Analysis and Realization of an Adaptive Isolator. Journal of Applied Mechanics, Transactions ASME, 2018, 85, .	2.2	7
311	An attenuation signal-based identification approach for parameters in weak nonlinear systems with asymmetry. International Journal of Non-Linear Mechanics, 2018, 99, 97-104.	2.6	8
312	Design of laser-driven SiO2-YAG:Ce composite thick film: Facile synthesis, robust thermal performance, and application in solid-state laser lighting. Optical Materials, 2018, 75, 508-512.	3.6	43
313	Nasal epithelial barrier disruption by particulate matter â‰ <b>2</b> .5 μm via tight junction protein degradation. Journal of Applied Toxicology, 2018, 38, 678-687.	2.8	78
314	Development and application of the diffusive gradients in thin films technique for simultaneous measurement of methcathinone and ephedrine in surface river water. Science of the Total Environment, 2018, 618, 284-290.	8.0	43
315	Investigation of an LuAC:Ce translucent ceramic synthesized via spark plasma sintering: Towards a facile synthetic route, robust thermal performance, and high-power solid state laser lighting. Journal of the European Ceramic Society, 2018, 38, 343-347.	5.7	78
316	Femtosecond laser induced selective etching in fused silica: optimization of the inscription conditions with a high-repetition-rate laser source. Optics Express, 2018, 26, 29669.	3.4	32
317	The Return of Ideology to China's Journalism Education: The †Joint Model' Campaign Between Propaganda Departments and Journalism Schools. Asia Pacific Media Educator, 2018, 28, 176-185.	0.5	3
318	Numerical Investigation of Coke Collapse and Size Segregation in the Bell-less Top Blast Furnace. ISIJ International, 2018, 58, 2018-2024.	1.4	14
319	1.2 μm persistent luminescence of Ho <sup>3+</sup> in LaAlO <sub>3</sub> and LaGaO <sub>3</sub> perovskites. Journal of Materials Chemistry C, 2018, 6, 11374-11383.	5.5	29
320	Axial Uplift Behaviour of Belled Piers in Coarse-Grained Saline Soils. Advances in Civil Engineering, 2018, 2018, 1-16.	0.7	1
321	Cow-to-mouse fecal transplantations suggest intestinal microbiome as one cause of mastitis. Microbiome, 2018, 6, 200.	11.1	88
322	Characteristics of Corporate R&D Investment in Emerging Markets: Evidence from Manufacturing Industry in China and South Korea. Sustainability, 2018, 10, 3002.	3.2	41
323	Identifying and Predicting Novelty in Microbiome Studies. MBio, 2018, 9, .	4.1	28
324	Impact of DNA extraction method and targeted 16S-rRNA hypervariable region on oral microbiota profiling. Scientific Reports, 2018, 8, 16321.	3.3	126

#	Article	IF	CITATIONS
325	Mechanism of slope failure in loess terrains during spring thawing. Journal of Mountain Science, 2018, 15, 845-858.	2.0	27
326	Intellectual Capital, Financial Performance and Companies' Sustainable Growth: Evidence from the Korean Manufacturing Industry. Sustainability, 2018, 10, 4651.	3.2	140
327	Long Low-Loss-Litium Niobate on Insulator Waveguides with Sub-Nanometer Surface Roughness. Nanomaterials, 2018, 8, 910.	4.1	113
328	Glassâ€Channel Molding Assisted 3D Printing of Metallic Microstructures Enabled by Femtosecond Laser Internal Processing and Microfluidic Electroless Plating. Advanced Materials Technologies, 2018, 3, 1800372.	5.8	16
329	3D Biomimetic Chips for Cancer Cell Migration in Nanometer-Sized Spaces Using "Ship-in-a-Bottle― Femtosecond Laser Processing. ACS Applied Bio Materials, 2018, 1, 1667-1676.	4.6	15
330	Expression, Purification, and Characterization of Recombinant Human α1-Antitrypsin Produced Using Silkworm–Baculovirus Expression System. Molecular Biotechnology, 2018, 60, 924-934.	2.4	15
331	Counteractive effects of regional transport and emission control on the formation of fine particles: a case study during the Hangzhou G20 summit. Atmospheric Chemistry and Physics, 2018, 18, 13581-13600.	4.9	43
332	A unique color converter geometry for laser-driven white lighting. Optical Materials, 2018, 86, 286-290.	3.6	8
333	Understanding the formation of interdisciplinary research from the perspective of keyword evolution: a case study on joint attention. Scientometrics, 2018, 117, 973-995.	3.0	32
334	Dynamic transport of antibiotics and antibiotic resistance genes under different treatment processes in a typical pharmaceutical wastewater treatment plant. Environmental Science and Pollution Research, 2018, 25, 30191-30198.	5.3	27
335	Ramanâ€∎ctivated cell sorting and metagenomic sequencing revealing carbonâ€fixing bacteria in the ocean. Environmental Microbiology, 2018, 20, 2241-2255.	3.8	62
336	Distributed Adaptive Synchronization Control with Friction Compensation of Networked Lagrange Systems. International Journal of Control, Automation and Systems, 2018, 16, 1038-1048.	2.7	6
337	Transcriptome analysis reveals the genetic foundation for the dynamics of starch and lipid production in Ettlia oleoabundans. Algal Research, 2018, 33, 142-155.	4.6	21
338	Constitutive activation of hedgehog signaling adversely affects epithelial cell fate during palatal fusion. Developmental Biology, 2018, 441, 191-203.	2.0	12
339	Mg <sub>2</sub> Nb <sub>34</sub> O <sub>87</sub> Porous Microspheres for Use in High-Energy, Safe, Fast-Charging, and Stable Lithium-Ion Batteries. ACS Applied Materials & Interfaces, 2018, 10, 23711-23720.	8.0	58
340	Template-free synthesis of bubble-like phosphorus-doped carbon nitride with enhanced visible-light photocatalytic activity. Journal of Alloys and Compounds, 2018, 769, 503-511.	5.5	32
341	Tailoring Trap Depth and Emission Wavelength in Y <sub>3</sub> Al <sub>5–<i>x</i></sub> Ga <i><sub>x</sub></i> O <sub>12</sub> :Ce <sup>3+</sup> ,V <sup Films for Optical Information Storage. ACS Applied Materials &amp; Interfaces, 2018, 10, 27150-27159.</sup 	>3+8 <b>.≬s</b> up	>Ph <b>89</b> phor-in-
342	The Impact of Government Subsidies on Private R&D and Firm Performance: Does Ownership Matter	3.2	63

in China's Manufacturing Industry?. Sustainability, 2018, 10, 2205.

#	Article	IF	CITATIONS
343	Thermodynamic, Structural and Thermoelectric Properties of AgSbTe2 Thick Films Developed by Melt Spinning. Nanomaterials, 2018, 8, 474.	4.1	10
344	Study of Phosphorus Removal by Using Sponge Iron Adsorption. Water, Air, and Soil Pollution, 2018, 229, 1.	2.4	14
345	Neural network control of networked redundant manipulator system with weight initialization method. Neurocomputing, 2018, 307, 117-129.	5.9	18
346	The aqueous corrosion of nuclear waste glasses revisited: Probing the surface and interfacial phenomena. Corrosion Science, 2018, 143, 65-75.	6.6	9
347	Stability and dynamics of parallel plunge grinding. International Journal of Advanced Manufacturing Technology, 2018, 99, 881-895.	3.0	19
348	A carbon nanotube-embedded conjugated polymer mesh with controlled oil absorption and surface regeneration via in situ wettability switch. Journal of Colloid and Interface Science, 2018, 532, 790-797.	9.4	9
349	Pressure effect on structural and electrical properties of AZO thin films annealed in N2/H2 atmosphere. Materials Letters, 2018, 232, 51-53.	2.6	8
350	A functional polypeptide N-acetylgalactosaminyltransferase (PGANT) initiates O-glycosylation in cultured silkworm BmN4 cells. Applied Microbiology and Biotechnology, 2018, 102, 8783-8797.	3.6	8
351	A novel isolation structure with flexible joints for impact and ultralow-frequency excitations. International Journal of Mechanical Sciences, 2018, 146-147, 366-376.	6.7	20
352	A vibration-driven planar locomotion robot— <i>Shell</i> . Robotica, 2018, 36, 1402-1420.	1.9	27
353	Privacy concerns in China's smart city campaign: The deficit of China's Cybersecurity Law. Asia and the Pacific Policy Studies, 2018, 5, 533-543.	1.5	23
354	Transient Interaction Between Reduction and Slagging Reactions of Wustite in Simulated Cohesive Zone of Blast Furnace. Metallurgical and Materials Transactions B: Process Metallurgy and Materials Processing Science, 2018, 49, 2308-2321.	2.1	10
355	Spatiotemporal profile of tetracycline and sulfonamide and their resistance on a catchment scale. Environmental Pollution, 2018, 241, 1098-1105.	7.5	26
356	Microscopic behavior and metallic iron morphology from reduction of iron oxide by CO/H <sub>2</sub> in a fluidized bed. Journal of Applied Crystallography, 2018, 51, 1641-1651.	4.5	17
357	Development of a facile droplet-based single-cell isolation platform for cultivation and genomic analysis in microorganisms. Scientific Reports, 2017, 7, 41192.	3.3	60
358	Two microporous Fe-based MOFs with multiple active sites for selective gas adsorption. Chemical Communications, 2017, 53, 2394-2397.	4.1	72
359	Study on the strength and deformation property of frozen silty sand with NaCl under tri-axial compression condition. Cold Regions Science and Technology, 2017, 137, 7-16.	3.5	11
360	Parallel-META 3: Comprehensive taxonomical and functional analysis platform for efficient comparison of microbial communities. Scientific Reports, 2017, 7, 40371.	3.3	96

#	Article	IF	CITATIONS
361	Photocatalytic removal of tetrabromobisphenol A by magnetically separable flower-like BiOBr/BiOl/Fe 3 O 4 hybrid nanocomposites under visible-light irradiation. Journal of Hazardous Materials, 2017, 331, 1-12.	12.4	147
362	Metabolic-Activity-Based Assessment of Antimicrobial Effects by D <sub>2</sub> O-Labeled Single-Cell Raman Microspectroscopy. Analytical Chemistry, 2017, 89, 4108-4115.	6.5	129
363	pH Switchable Emulsions Based on Dynamic Covalent Surfactants. Langmuir, 2017, 33, 3040-3046.	3.5	51
364	Controllable alignment of elongated microorganisms in 3D microspace using electrofluidic devices manufactured by hybrid femtosecond laser microfabrication. Microsystems and Nanoengineering, 2017, 3, 16078.	7.0	28
365	Oridonin inhibition and miR-200b-3p/ZEB1 axis in human pancreatic cancer. International Journal of Oncology, 2017, 50, 111-120.	3.3	33
366	A Niccolite Structural Multiferroic Metal–Organic Framework Possessing Four Different Types of Bistability in Response to Dielectric and Magnetic Modulation. Advanced Materials, 2017, 29, 1606966.	21.0	107
367	Toward tunable and bright deepâ€red persistent luminescence of Cr <sup>3+</sup> in garnets. Journal of the American Ceramic Society, 2017, 100, 4033-4044.	3.8	70
368	Nonlinear equivalent model and its identification for a delayed absorber with magnetic action using distorted measurement. Nonlinear Dynamics, 2017, 88, 937-954.	5.2	12
369	Celebrity-inspired, Fan-driven: Doing Philanthropy through Social Media in Mainland China. Asian Studies Review, 2017, 41, 244-262.	1.1	15
370	T-Helper Type 1-T-Helper Type 2 Shift and Nasal Remodeling after Fine Particulate Matter Exposure in a Rat Model of Allergic Rhinitis. American Journal of Rhinology and Allergy, 2017, 31, 148-155.	2.0	29
371	Characterization of Recombinant Thermococcus kodakaraensis (KOD) DNA Polymerases Produced Using Silkworm-Baculovirus Expression Vector System. Molecular Biotechnology, 2017, 59, 221-233.	2.4	13
372	Interfacial Growth of TiO <sub>2</sub> -rGO Composite by Pickering Emulsion for Photocatalytic Degradation. Langmuir, 2017, 33, 5015-5024.	3.5	54
373	Signal Transductions of BEAS-2B Cells in Response to Carcinogenic PM <sub>2.5</sub> Exposure Based on a Microfluidic System. Analytical Chemistry, 2017, 89, 5413-5421.	6.5	42
374	Investigation of the fiber <scp>B</scp> ragg grating inscribed in multimode fiber by femtosecond laser. Microwave and Optical Technology Letters, 2017, 59, 214-219.	1.4	3
375	Desynchronization-based congestion suppression for a star-type Internet system with arbitrary dimension. Neurocomputing, 2017, 266, 42-55.	5.9	11
376	Experiment-based identification of time delays in linear systems. Acta Mechanica Sinica/Lixue Xuebao, 2017, 33, 429-439.	3.4	5
377	Expression and Characterization of Human β-1, 4-Galactosyltransferase 1 (β4GalT1) Using Silkworm–Baculovirus Expression System. Molecular Biotechnology, 2017, 59, 151-158.	2.4	13
378	Ore fluid evolution in the giant Marcona Fe-(Cu) deposit, Perú: Evidence from in-situ sulfur isotope and trace element geochemistry of sulfides. Ore Geology Reviews, 2017, 86, 624-638.	2.7	16

#	Article	IF	CITATIONS
379	Emerging Trends for Microbiome Analysis: From Single-Cell Functional Imaging to Microbiome Big Data. Engineering, 2017, 3, 66-70.	6.7	30
380	Maximizing the Density of Active Groups in Porous Poly(ionic liquids) for Efficient Adsorptive Desulfurization. Industrial & Engineering Chemistry Research, 2017, 56, 4319-4326.	3.7	9
381	Thermoluminescence investigation on Y 3 Al 5 â^'x Ga x O 12 :Ce 3+ -Bi 3+ green persistent phosphors. Journal of Luminescence, 2017, 183, 355-359.	3.1	27
382	Fabrication of one-dimensional Bi <sub>2</sub> O <sub>3</sub> –Bi <sub>14</sub> MoO <sub>24</sub> heterojunction photocatalysts with high interface quality. CrystEngComm, 2017, 19, 237-245.	2.6	20
383	Assessing the photocatalytic transformation of norfloxacin by BiOBr/iron oxides hybrid photocatalyst: Kinetics, intermediates, and influencing factors. Applied Catalysis B: Environmental, 2017, 205, 68-77.	20.2	145
384	Producing Designer Oils in Industrial Microalgae by Rational Modulation of Co-evolving Type-2 Diacylglycerol Acyltransferases. Molecular Plant, 2017, 10, 1523-1539.	8.3	111
385	DLX3 promotes bone marrow mesenchymal stem cell proliferation through H19/miR-675 axis. Clinical Science, 2017, 131, 2721-2735.	4.3	15
386	Controlled synthesis of one-dimensional BiOBr with exposed (110) facets and enhanced photocatalytic activity. CrystEngComm, 2017, 19, 6473-6480.	2.6	60
387	Basins of attraction of the bistable region of time-delayed cutting dynamics. Physical Review E, 2017, 96, 032205.	2.1	20
388	Enhancing photosynthetic biomass productivity of industrial oleaginous microalgae by overexpression of RuBisCO activase. Algal Research, 2017, 27, 366-375.	4.6	99
389	Transition sets analysis based parametrical design of nonlinear metal rubber isolator. International Journal of Non-Linear Mechanics, 2017, 96, 93-105.	2.6	10
390	Influence of Workpiece Imbalance on Regenerative and Frictional Grinding Chatters. Procedia IUTAM, 2017, 22, 146-153.	1.2	8
391	Br-Doped Bi <sub>2</sub> O <sub>2</sub> CO <sub>3</sub> exposed (001) crystal facets with enhanced photocatalytic activity. CrystEngComm, 2017, 19, 5001-5007.	2.6	36
392	Investigation and Application of a New Passive Sampling Technique for in Situ Monitoring of Illicit Drugs in Waste Waters and Rivers. Environmental Science & Technology, 2017, 51, 9101-9108.	10.0	68
393	Analysis of worm-like locomotion driven by the sine-squared strain wave in a linear viscous medium. Mechanics Research Communications, 2017, 85, 33-44.	1.8	11
394	Ecological Effect of Arginine on Oral Microbiota. Scientific Reports, 2017, 7, 7206.	3.3	46
395	Cr <sup>3+</sup> /Er <sup>3+</sup> co-doped LaAlO <sub>3</sub> perovskite phosphor: a near-infrared persistent luminescence probe covering the first and third biological windows. Journal of Materials Chemistry B, 2017, 5, 6385-6393.	5.8	65
396	<i>The Internet and New Social Formation in China: Fandom Publics in the Making</i> , by Weiyu Zhang. London: Routledge, 2016. x+143 pp. £90.00 (cloth) China Journal, 2017, 78, 161-162.	0.2	0

#	Article	IF	CITATIONS
397	SUMOylation regulates the localization and activity of Polo-like kinase 1 during cell cycle in the silkworm, Bombyx mori. Scientific Reports, 2017, 7, 15536.	3.3	9
398	Facet-selective interface design of a BiOl <sub>(110)</sub> /Br-Bi <sub>2</sub> O <sub>2</sub> CO <sub>3(110)</sub> p–n heterojunction photocatalyst. CrystEngComm, 2017, 19, 6837-6844.	2.6	14
399	A Noise Correction Embedded Identification Approach for Delays and Parameters in Nonlinear Delay Systems. Procedia IUTAM, 2017, 22, 67-74.	1.2	4
400	Raman-Activated Droplet Sorting (RADS) for Label-Free High-Throughput Screening of Microalgal Single-Cells. Analytical Chemistry, 2017, 89, 12569-12577.	6.5	113
401	Regenerative chatter in a plunge grinding process with workpiece imbalance. International Journal of Advanced Manufacturing Technology, 2017, 89, 2845-2862.	3.0	19
402	Red persistent luminescence in rare earth-free AlN:Mn2+ phosphor. Materials Letters, 2017, 206, 175-177.	2.6	28
403	<scp>RNA</scp> iâ€based targeted gene knockdown in the model oleaginous microalgae <i>Nannochloropsis oceanica</i> . Plant Journal, 2017, 89, 1236-1250.	5.7	74
404	Zero-Hopf bifurcation and multistability coexistence on a four-neuron network model with multiple delays. Nonlinear Dynamics, 2017, 87, 2357-2366.	5.2	12
405	H2O2 and/or TiO2 photocatalysis under UV irradiation for the removal of antibiotic resistant bacteria and their antibiotic resistance genes. Journal of Hazardous Materials, 2017, 323, 710-718.	12.4	134
406	The effect and design of time delay in feedback control for a nonlinear isolation system. Mechanical Systems and Signal Processing, 2017, 87, 206-217.	8.0	56
407	<i>Shanzhai</i> Media Culture: Failed Intervention to the Disingenuous Neoliberal Logic of Chinese Media. Journal of Contemporary China, 2017, 26, 249-262.	2.3	6
408	Influence of nonlinearity on transition curves in a parametric pendulum system. Communications in Nonlinear Science and Numerical Simulation, 2017, 42, 275-284.	3.3	6
409	Effect of the selective pressure of sub-lethal level of heavy metals on the fate and distribution of ARGs in the catchment scale. Environmental Pollution, 2017, 220, 900-908.	7.5	144
410	Drugs of abuse and their metabolites in the urban rivers of Beijing, China: Occurrence, distribution, and potential environmental risk. Science of the Total Environment, 2017, 579, 305-313.	8.0	58
411	A novel 3D hollow magnetic Fe3O4/BiOI heterojunction with enhanced photocatalytic performance for bisphenol A degradation. Chemical Engineering Journal, 2017, 307, 1055-1065.	12.7	135
412	Ultrafast Laser Fabrication of Functional Biochips: New Avenues for Exploring 3D Micro- and Nano-Environments. Micromachines, 2017, 8, 40.	2.9	18
413	Evidence of valence state change of Ce^3+ and Cr^3+ during UV charging process in Y_3Al_2Ga_3O_12 persistent phosphors. Optical Materials Express, 2017, 7, 2471.	3.0	24
414	The Optimal Locomotion of a Self-Propelled Worm Actuated by Two Square Waves. Micromachines, 2017, 8, 364.	2.9	2

#	Article	IF	CITATIONS
415	PM2.5-Induced Oxidative Stress and Mitochondrial Damage in the Nasal Mucosa of Rats. International Journal of Environmental Research and Public Health, 2017, 14, 134.	2.6	76
416	Metabolic Remodeling of Membrane Glycerolipids in the Microalga Nannochloropsis oceanica under Nitrogen Deprivation. Frontiers in Marine Science, 2017, 4, .	2.5	45
417	Label-free, simultaneous quantification of starch, protein and triacylglycerol in single microalgal cells. Biotechnology for Biofuels, 2017, 10, 275.	6.2	44
418	Feed-additive probiotics accelerate yet antibiotics delay intestinal microbiota maturation in broiler chicken. Microbiome, 2017, 5, 91.	11.1	208
419	Genomic Analysis of Glutathione S-transferases (GST) Family in Common Carp: Identification, Phylogeny and Expression. Pakistan Journal of Zoology, 2017, 49, 1437-1448.	0.2	5
420	Numerical simulation for Human Quiet Standing System. MATEC Web of Conferences, 2016, 61, 01021.	0.2	0
421	The First Demonstration of the Gyroid in a Polyoxometalateâ€Based Open Framework with High Proton Conductivity. Chemistry - A European Journal, 2016, 22, 9082-9086.	3.3	37
422	Author creditâ€assignment schemas: A comparison and analysis. Journal of the Association for Information Science and Technology, 2016, 67, 1973-1989.	2.9	25
423	CRISPR/Cas9-mediated knockout of factors in non-homologous end joining pathway enhances gene targeting in silkworm cells. Scientific Reports, 2016, 5, 18103.	3.3	40
424	Senescence: novel insight into DLX3 mutations leading to enhanced bone formation in Tricho-Dento-Osseous syndrome. Scientific Reports, 2016, 6, 38680.	3.3	12
425	High-level expression and purification of biologically active human IL-2 using silkworm-baculovirus expression vector system. Journal of Asia-Pacific Entomology, 2016, 19, 313-317.	0.9	14
426	Synthesis and photoluminescent properties of Sr(1â°'x)Si2O2N2: xEu2+ phosphor prepared by polymer metal complex method for WLEDs applications. Materials Research Bulletin, 2016, 79, 69-72.	5.2	8
427	A novel cleaner production process of citric acid by recycling its treated wastewater. Bioresource Technology, 2016, 211, 645-653.	9.6	13
428	A novel stepwise pretreatment on corn stalk by alkali deacetylation and liquid hot water for enhancing enzymatic hydrolysis and energy utilization efficiency. Bioresource Technology, 2016, 209, 115-124.	9.6	27
429	Occurrence and distribution of antibiotics, antibiotic resistance genes in the urban rivers in Beijing, China. Environmental Pollution, 2016, 213, 833-840.	7.5	226
430	Photostimulation induced persistent luminescence in Y_3Al_2Ga_3O_12:Cr^3+. Optical Materials Express, 2016, 6, 1405.	3.0	63
431	Vibration control of nonlinear Absorber–Isolator-Combined structure with time-delayed coupling. International Journal of Non-Linear Mechanics, 2016, 83, 48-58.	2.6	16

432 Locking mechanisms in degree-4 vertex origami structures. , 2016, , .

#	Article	IF	CITATIONS
433	Novel persistent phosphors of lanthanide–chromium co-doped yttrium aluminum gallium garnet: design concept with vacuum referred binding energy diagram. Journal of Materials Chemistry C, 2016, 4, 4380-4386.	5.5	49
434	Reverse and Multiple Stable Isotope Probing to Study Bacterial Metabolism and Interactions at the Single Cell Level. Analytical Chemistry, 2016, 88, 9443-9450.	6.5	72
435	Bioassay-directed identification of toxicants in sediments of Liaohe River, northeast China. Environmental Pollution, 2016, 219, 663-671.	7.5	12
436	Co-expression of silkworm allatostatin-C receptor BNGR-A1 with its cognate G protein subunits enhances the GPCR display on the budding baculovirus. Journal of Asia-Pacific Entomology, 2016, 19, 753-760.	0.9	3
437	Cetylpyridinium chloride mouth rinses alleviate experimental gingivitis by inhibiting dental plaque maturation. International Journal of Oral Science, 2016, 8, 182-190.	8.6	41
438	Role of synthesis method and α, β-Sr (2-x) SiO 4 : xEu 2+ phases on the photoluminescent properties of Sr (1-x) Si 2 O 2 N 2 : xEu 2+ phosphors. Materials Research Bulletin, 2016, 83, 468-473.	5.2	5
439	Proteasome inhibitor MG132 impairs autophagic flux through compromising formation of autophagosomes in Bombyx cells. Biochemical and Biophysical Research Communications, 2016, 479, 690-696.	2.1	13
440	Lateral periodic vibrations of footbridges under crowd excitation. Nonlinear Dynamics, 2016, 86, 1701-1710.	5.2	5
441	Scintillation and optical properties of Ce-doped YAGG transparent ceramics. Journal of Rare Earths, 2016, 34, 763-768.	4.8	17
442	Genome editing of model oleaginous microalgae <i>Nannochloropsis</i> spp. by <scp>CRISPR</scp> /Cas9. Plant Journal, 2016, 88, 1071-1081.	5.7	229
443	Airborne Fine Particulate Matter Induces Oxidative Stress and Inflammation in Human Nasal Epithelial Cells. Tohoku Journal of Experimental Medicine, 2016, 239, 117-125.	1.2	110
444	A Rigid Nested Metal–Organic Framework Featuring a Thermoresponsive Gating Effect Dominated by Counterions. Angewandte Chemie, 2016, 128, 15251-15254.	2.0	16
445	Intestinal Microbiota Distinguish Gout Patients from Healthy Humans. Scientific Reports, 2016, 6, 20602.	3.3	238
446	Comparative study of optical and scintillation properties of Ce:YAGG, Ce:GAGG and Ce:LuAGG transparent ceramics. Journal of the Ceramic Society of Japan, 2016, 124, 569-573.	1.1	25
447	The adsorption behaviors of CO and H2 on FeO surface: A density functional theory study. Powder Technology, 2016, 303, 100-108.	4.2	35
448	Time-delay identification for vibration systems with multiple feedback. Acta Mechanica Sinica/Lixue Xuebao, 2016, 32, 1138-1148.	3.4	2
449	A Comparison on Ce <sup>3+</sup> Luminescence in Borate Class and YAG Ceramic: Understanding the Role of Host's Characteristics. Journal of Physical Chemistry C, 2016, 120, 17683-17691.	3.1	51
450	The time-delay coupling nonlinear effect in sky-hook control of vibration isolation systems using Magneto-Rheological Fluid dampers. Journal of Mechanical Science and Technology, 2016, 30, 4157-4166.	1.5	7

#	Article	IF	CITATIONS
451	Microbiota-based Signature of Gingivitis Treatments: A Randomized Study. Scientific Reports, 2016, 6, 24705.	3.3	27
452	Diversity and resilience of the woodâ€feeding higher termite <i>Mironasutitermes shangchengensis</i> gut microbiota in response to temporal and diet variations. Ecology and Evolution, 2016, 6, 8235-8242.	1.9	23
453	A Rigid Nested Metal–Organic Framework Featuring a Thermoresponsive Gating Effect Dominated by Counterions. Angewandte Chemie - International Edition, 2016, 55, 15027-15030.	13.8	166
454	Label-free, rapid and quantitative phenotyping of stress response in E. coli via ramanome. Scientific Reports, 2016, 6, 34359.	3.3	87
455	Study on Trap Levels in SrSi <sub>2</sub> AlO <sub>2</sub> N <sub>3</sub> :Eu <sup>2+</sup> ,Ln <sup>3+</sup> Persistent Phosphors Based on Host-Referred Binding Energy Scheme and Thermoluminescence Analysis. Inorganic Chemistry. 2016. 55. 11890-11897.	4.0	47
456	Near-infrared long persistent luminescence of Er <sup>3+</sup> in garnet for the third bio-imaging window. Journal of Materials Chemistry C, 2016, 4, 11096-11103.	5.5	87
457	Regenerative chatter in self-interrupted plunge grinding. Meccanica, 2016, 51, 3185-3202.	2.0	17
458	Miniaturized fiber Fabry-Pérot interferometer for strain sensing. Microwave and Optical Technology Letters, 2016, 58, 1510-1514.	1.4	7
459	Stability switches and bifurcation analysis in a coupled neural system with multiple delays. Science China Technological Sciences, 2016, 59, 920-931.	4.0	6
460	Regenerative and frictional chatter in plunge grinding. Nonlinear Dynamics, 2016, 86, 283-307.	5.2	24
461	Construction of a polyhedron decorated MOF with a unique network through the combination of two classic secondary building units. Chemical Communications, 2016, 52, 2079-2082.	4.1	36
462	Structural stabilization of a metal–organic framework for gas sorption investigation. Dalton Transactions, 2016, 45, 6830-6833.	3.3	21
463	Effects of hydroxy propyl cellulose (HPC) surfactant on fabrication, microstructure and optical properties of Ce3+:Lu3Al5O12 (Ce:LuAG) transparent ceramics. Advanced Powder Technology, 2016, 27, 610-617.	4.1	3
464	Spatial distribution and potential toxicity of polycyclic aromatic hydrocarbons in sediments from Liaohe River Basin, China. Environmental Monitoring and Assessment, 2016, 188, 193.	2.7	19
465	Lu 3 Al 5 O 12 :Ce@SiO 2 phosphor-in-glass: Its facile synthesis, reduced thermal/chemical degradation and application in high-power white LEDs. Journal of the European Ceramic Society, 2016, 36, 2017-2025.	5.7	31
466	Sediment PAH source apportionment in the Liaohe River using the ME2 approach: A comparison to the PMF model. Science of the Total Environment, 2016, 553, 164-171.	8.0	37
467	Thermal management for high power lithium-ion battery by minichannel aluminum tubes. Applied Thermal Engineering, 2016, 101, 284-292.	6.0	232
468	Effect of propionic acid on citric acid fermentation in an integrated citric acid–methane fermentation process. Bioprocess and Biosystems Engineering, 2016, 39, 391-400.	3.4	9

#	Article	IF	CITATIONS
469	Preparation of electrospun YAG:Ce nanofiber-based phosphor layer for white LEDs application. Ceramics International, 2016, 42, 4616-4620.	4.8	15
470	Effect of structures and sunny–shady slopes on thermal characteristics of subgrade along the Harbin–Dalian Passenger Dedicated Line in Northeast China. Cold Regions Science and Technology, 2016, 123, 14-21.	3.5	66
471	A chiral lanthanide metal–organic framework for selective sensing of Fe( <scp>iii</scp> ) ions. Dalton Transactions, 2016, 45, 1040-1046.	3.3	269
472	Time delay identifiability and estimation for the delayed linear system with incomplete measurement. Journal of Sound and Vibration, 2016, 361, 330-340.	3.9	9
473	Planar locomotion of a vibration-driven system with two internal masses. Applied Mathematical Modelling, 2016, 40, 871-885.	4.2	20
474	A three-phase vibration-driven system's locomotion on an isotropic rough surface. , 2015, , .		1
475	Anionâ€Triggered Modulation of Structure and Magnetic Properties of Copper(I)–Dysprosium(III) Complexes Derived from 1â€Hydroxybenzotriazolate. European Journal of Inorganic Chemistry, 2015, 2015, 5379-5386.	2.0	11
476	Lateral Vibrations of a Cable-Stayed Bridge under Crowd Excitation. Mathematical Problems in Engineering, 2015, 2015, 1-11.	1.1	0
477	Synchronization Transition and Traffic Congestion in One-Dimensional Traffic Model. Abstract and Applied Analysis, 2015, 2015, 1-10.	0.7	2
478	Oridonin inhibits BxPC-3 cell growth through cell apoptosis. Acta Biochimica Et Biophysica Sinica, 2015, 47, 164-173.	2.0	25
479	Preparation Eu-doped ca-α-SiAlON phosphor by heterogeneous precipitation: An orange–yellow phosphor for white light-emitting diodes. Ceramics International, 2015, 41, 11086-11090.	4.8	15
480	Spatial distribution and toxicity assessment of heavy metals in sediments of Liaohe River, northeast China. Environmental Science and Pollution Research, 2015, 22, 14960-14970.	5.3	14
481	Locomotion analysis of a vibration-driven system with three acceleration-controlled internal masses. Advances in Mechanical Engineering, 2015, 7, 168781401557376.	1.6	8
482	Human alpha 1-acid glycoprotein as a model protein for glycoanalysis in baculovirus expression vector system. Journal of Asia-Pacific Entomology, 2015, 18, 303-309.	0.9	11
483	Multitype Activity Coexistence in an Inertial Two-Neuron System with Multiple Delays. International Journal of Bifurcation and Chaos in Applied Sciences and Engineering, 2015, 25, 1530040.	1.7	36
484	Flavin mononucleotide (FMN)-based fluorescent protein (FbFP) as reporter for promoter screening in Clostridium cellulolyticum. Journal of Microbiological Methods, 2015, 119, 37-43.	1.6	26
485	Syntheses, structures and magnetic properties of Fe6 and Fe12 ferric wheels. Science China Chemistry, 2015, 58, 1853-1857.	8.2	8
486	Phase coordination and phase–velocity relationship in metameric robot locomotion. Bioinspiration and Biomimetics, 2015, 10, 066006.	2.9	55

#	Article	IF	CITATIONS
487	An introduction and guidance for neurodynamics. Science Bulletin, 2015, 60, 1969-1971.	9.0	25
488	In-channel integration of designable microoptical devices using flat scaffold-supported femtosecond-laser microfabrication for coupling-free optofluidic cell counting. Light: Science and Applications, 2015, 4, e228-e228.	16.6	107
489	Experiments and analysis for a controlled mechanical absorber considering delay effect. Journal of Sound and Vibration, 2015, 339, 25-37.	3.9	46
490	Improvement of Endo-β-N-acetylglucosaminidase H production using silkworm–baculovirus protein expression system. Journal of Asia-Pacific Entomology, 2015, 18, 175-180.	0.9	12
491	Synthesis and characterization of magnetically recyclable Ag nanoparticles immobilized on Fe3O4@C nanospheres with catalytic activity. Applied Surface Science, 2015, 335, 23-28.	6.1	39
492	Non-linear analysis and quench control of chatter in plunge grinding. International Journal of Non-Linear Mechanics, 2015, 70, 134-144.	2.6	23
493	Phytohormones in microalgae: a new opportunity for microalgal biotechnology?. Trends in Plant Science, 2015, 20, 273-282.	8.8	268
494	Single cell biotechnology to shed a light on biological â€~dark matter' in nature. Microbial Biotechnology, 2015, 8, 15-16.	4.2	20
495	Raman-Activated Cell Sorting Based on Dielectrophoretic Single-Cell Trap and Release. Analytical Chemistry, 2015, 87, 2282-2289.	6.5	126
496	Ship-in-a-bottle femtosecond laser integration of optofluidic microlens arrays with center-pass units enabling coupling-free parallel cell counting with a 100% success rate. Lab on A Chip, 2015, 15, 1515-1523.	6.0	64
497	Pitchfork and octopus bifurcations in a hyperelastic tube subjected to compression: Analytical post-bifurcation solutions and imperfection sensitivity. Mathematics and Mechanics of Solids, 2015, 20, 25-52.	2.4	13
498	Biochemical characterization of maintenance DNA methyltransferase DNMT-1 from silkworm, Bombyx mori. Insect Biochemistry and Molecular Biology, 2015, 58, 55-65.	2.7	22
499	Comparison on structural modification of industrial lignin by wet ball milling and ionic liquid pretreatment. Biotechnology Reports (Amsterdam, Netherlands), 2015, 6, 1-7.	4.4	57
500	A 3-D Quasi-Zero-Stiffness-Based Sensor System for Absolute Motion Measurement and Application in Active Vibration Control. IEEE/ASME Transactions on Mechatronics, 2015, 20, 254-262.	5.8	28
501	Optimization of the integrated citric acid–methane fermentation process by air stripping and glucoamylase addition. Bioprocess and Biosystems Engineering, 2015, 38, 411-420.	3.4	7
502	A comprehensive study on the locomotion characteristics of a metameric earthworm-like robot. Multibody System Dynamics, 2015, 35, 153-177.	2.7	46
503	Polybrominated diphenyl ethers (PBDEs) and polychlorinated biphenyls (PCBs) in sediments of Liaohe River: levels, spatial and temporal distribution, possible sources, and inventory. Environmental Science and Pollution Research, 2015, 22, 4256-4264.	5.3	41
504	Fabrication of Ce3+–Cr3+ co-doped yttrium aluminium gallium garnet transparent ceramic phosphors with super long persistent luminescence. Scripta Materialia, 2015, 102, 47-50.	5.2	95

#	Article	IF	CITATIONS
505	A comprehensive study on the locomotion characteristics of a metameric earthworm-like robot. Multibody System Dynamics, 2015, 34, 391-413.	2.7	27
506	A multi-directional vibration isolator based on Quasi-Zero-Stiffness structure and time-delayed active control. International Journal of Mechanical Sciences, 2015, 100, 126-135.	6.7	68
507	Sr1.98Eu0.02SiO4 luminescence whisker based on vapor-phase deposition: Facile synthesis, uniform morphology and enhanced luminescence properties. Materials Research Bulletin, 2015, 71, 106-110.	5.2	3
508	Multiple pitchfork bifurcations and multiperiodicity coexistences in a delay-coupled neural oscillator system with inhibitory-to-inhibitory connection. Communications in Nonlinear Science and Numerical Simulation, 2015, 29, 327-345.	3.3	21
509	Comparative proteomic analysis of hemolymph proteins from Autographa californica multiple nucleopolyhedrovirus (AcMNPV)-sensitive or -resistant silkworm strains during infections. Comparative Biochemistry and Physiology Part D: Genomics and Proteomics, 2015, 16, 36-47.	1.0	9
510	Two Gd <sup>III</sup> complexes derived from dicarboxylate ligands as cryogenic magnetorefrigerants. New Journal of Chemistry, 2015, 39, 6970-6975.	2.8	52
511	Ln <sup>III</sup> ion dependent magnetism in heterometallic Cu–Ln complexes based on an azido group and 1,2,3-triazole-4,5-dicarboxylate as co-ligands. RSC Advances, 2015, 5, 62319-62324.	3.6	7
512	Loqs depends on R2D2 to localize in D2 body-like granules and functions in RNAi pathways in silkworm cells. Insect Biochemistry and Molecular Biology, 2015, 64, 78-90.	2.7	5
513	Cleaner production of citric acid by recycling its extraction wastewater treated with anaerobic digestion and electrodialysis in an integrated citric acid–methane production process. Bioresource Technology, 2015, 189, 186-194.	9.6	22
514	Mass Production of an Active Peptide-N-Glycosidase F Using Silkworm-Baculovirus Expression System. Molecular Biotechnology, 2015, 57, 735-745.	2.4	16
515	Application of Metaâ€Mesh on the analysis of microbial communities from human associatedâ€habitats. Quantitative Biology, 2015, 3, 4-18.	0.5	2
516	Distribution, source characterization and inventory of perfluoroalkyl substances in Taihu Lake, China. Chemosphere, 2015, 127, 201-207.	8.2	58
517	Oridonin alters the expression profiles of MicroRNAs in BxPC-3 human pancreatic cancer cells. BMC Complementary and Alternative Medicine, 2015, 15, 117.	3.7	18
518	Topological modulation of metal–thiadiazole dicarboxylate coordination polymers through auxiliary ligand alteration. CrystEngComm, 2015, 17, 4301-4308.	2.6	10
519	Cellulosome stoichiometry in Clostridium cellulolyticum is regulated by selective RNA processing and stabilization. Nature Communications, 2015, 6, 6900.	12.8	43
520	Experimental studies on active control of a dynamic system via a time-delayed absorber. Acta Mechanica Sinica/Lixue Xuebao, 2015, 31, 229-247.	3.4	29
521	A self-powered microfluidic monodispersed droplet generator with capability of multi-sample introduction. Microfluidics and Nanofluidics, 2015, 18, 1067-1073.	2.2	16
522	Y <sub>3</sub> Al <sub>5â^'</sub> <i><sub>x</sub></i> Ga <i><sub>x</sub></i> O <sub>12</sub> :Cr <sup>3+A novel red persistent phosphor with high brightness. Applied Physics Express, 2015, 8, 042602.</sup>	<sup>1</sup> ٣ <u>2:</u> 4	64

#	Article	IF	CITATIONS
523	Analysis of a Car-Following Model with Driver Memory Effect. International Journal of Bifurcation and Chaos in Applied Sciences and Engineering, 2015, 25, 1550057.	1.7	3
524	Vertical sidewall electrodes monolithically integrated into 3D glass microfluidic chips using water-assisted femtosecond-laser fabrication for in situ control of electrotaxis. RSC Advances, 2015, 5, 24072-24080.	3.6	93
525	Near-infrared multi-wavelengths long persistent luminescence of Nd3+ ion through persistent energy transfer in Ce3+, Cr3+ co-doped Y3Al2Ga3O12 for the first and second bio-imaging windows. Applied Physics Letters, 2015, 107, .	3.3	87
526	Design of deep-red persistent phosphors of Gd_3Al_5-xGa_xO_12:Cr^3+ transparent ceramics sensitized by Eu^3+ as an electron trap using conduction band engineering. Optical Materials Express, 2015, 5, 963.	3.0	45
527	Genomic Foundation of Starch-to-Lipid Switch in Oleaginous <i>Chlorella</i> spp Plant Physiology, 2015, 169, 2444-2461.	4.8	111
528	Novel Lead-free Glass/Ceramics System with Low Permittivity, Low Loss for LTCC Application. International Journal of Applied Ceramic Technology, 2015, 12, E112-E116.	2.1	6
529	Roles of silkworm endoplasmic reticulum chaperones in the secretion of recombinant proteins expressed by baculovirus system. Molecular and Cellular Biochemistry, 2015, 409, 255-262.	3.1	10
530	Double Hopf bifurcation in a four-neuron delayed system with inertial terms. Nonlinear Dynamics, 2015, 82, 1969-1978.	5.2	7
531	Structure modulation in zinc–ditetrazolate coordination polymers by in situ ligand synthesis. RSC Advances, 2015, 5, 88809-88815.	3.6	6
532	Pattern dynamics of a predator–prey reaction–diffusion model with spatiotemporal delay. Nonlinear Dynamics, 2015, 81, 2155-2163.	5.2	26
533	Towards high-throughput microfluidic Raman-activated cell sorting. Analyst, The, 2015, 140, 6163-6174.	3.5	67
534	An improved time-delay saturation controller for suppression of nonlinear beam vibration. Nonlinear Dynamics, 2015, 82, 1691-1707.	5.2	17
535	Prediction of Early Childhood Caries via Spatial-Temporal Variations of Oral Microbiota. Cell Host and Microbe, 2015, 18, 296-306.	11.0	204
536	Probing the severe haze pollution in three typical regions of China: Characteristics, sources and regional impacts. Atmospheric Environment, 2015, 120, 76-88.	4.1	106
537	Delay-Induced Bogdanov–Takens Bifurcation and Dynamical Classifications in a Slow-Fast Flexible Joint System. International Journal of Bifurcation and Chaos in Applied Sciences and Engineering, 2015, 25, 1550121.	1.7	4
538	Molecular mechanisms for photosynthetic carbon partitioning into storage neutral lipids in Nannochloropsis oceanica under nitrogen-depletion conditions. Algal Research, 2015, 7, 66-77.	4.6	188
539	Establishment and assessment of an integrated citric acid–methane production process. Bioresource Technology, 2015, 176, 121-128.	9.6	12
540	Occurrence of antibiotics and antibiotic resistance genes in a sewage treatment plant and its effluent-receiving river. Chemosphere, 2015, 119, 1379-1385.	8.2	524

#	Article	IF	CITATIONS
541	On the stability and multi-stability of a TCP/RED congestion control model with state-dependent delay and discontinuous marking function. Communications in Nonlinear Science and Numerical Simulation, 2015, 22, 269-284.	3.3	19
542	Precise quantitative addition of multiple reagents into droplets in sequence using glass fiber-induced droplet coalescence. Analyst, The, 2015, 140, 701-705.	3.5	0
543	Magnetic nanoparticle-mediated isolation of functional bacteria in a complex microbial community. ISME Journal, 2015, 9, 603-614.	9.8	75
544	Analysis of spatiotemporal patterns in a single species reaction–diffusion model with spatiotemporal delay. Nonlinear Analysis: Real World Applications, 2015, 22, 54-65.	1.7	15
545	Effect of oridonin-mediated hallmark changes on inflammatory pathways in human pancreatic cancer (BxPC-3) cells. World Journal of Gastroenterology, 2014, 20, 14895.	3.3	21
546	Saliva Microbiota Carry Caries-Specific Functional Gene Signatures. PLoS ONE, 2014, 9, e76458.	2.5	16
547	Analysis of Critical Velocities for an Infinite Timoshenko Beam Resting on an Elastic Foundation Subjected to a Harmonic Moving Load. Shock and Vibration, 2014, 2014, 1-9.	0.6	2
548	Intracellular Distributing and Interferon-Î <sup>3</sup> Secretion of Human Interleukin-18 in BxPC-3 Cells. International Journal of Medical Sciences, 2014, 11, 172-179.	2.5	0
549	Experimental observation of spike, burst and chaos synchronization of calcium concentration oscillations. Europhysics Letters, 2014, 106, 50003.	2.0	23
550	A carbon-free sol–gel method for preparation of Lu 3 Al 5 O 12 : Ce 3+ phosphors for potential applications in laser scintillators and LEDs. Materials Letters, 2014, 133, 1-4.	2.6	20
551	Consolidation of translucent Ce <sup>3+</sup> -doped Lu <sub>2</sub> SiO <sub>5</sub> scintillation ceramics by pressureless sintering. Journal of Materials Research, 2014, 29, 2252-2259.	2.6	9
552	A three-dimensional metal–organic framework for selective sensing of nitroaromatic compounds. APL Materials, 2014, 2, .	5.1	44
553	Stick-Slip Effect in a Vibration-Driven System With Dry Friction: Sliding Bifurcations and Optimization. Journal of Applied Mechanics, Transactions ASME, 2014, 81, .	2.2	47
554	On-demand control of microfluidic flow via capillary-tuned solenoid microvalve suction. Lab on A Chip, 2014, 14, 4599-4603.	6.0	19
555	Nannochloropsis Genomes Reveal Evolution of Microalgal Oleaginous Traits. PLoS Genetics, 2014, 10, e1004094.	3.5	217
556	Design and experimental gait analysis of a multi-segment in-pipe robot inspired by earthworm's peristaltic locomotion. Proceedings of SPIE, 2014, , .	0.8	4
557	Hybrid femtosecond laser microfabrication to achieve true 3D glass/polymer composite biochips with multiscale features and high performance: the concept of shipâ€inâ€aâ€bottle biochip. Laser and Photonics Reviews, 2014, 8, 458-467.	8.7	126
558	Effect of acetylation/deacetylation on enzymatic hydrolysis of corn stalk. Biomass and Bioenergy, 2014, 71, 294-298.	5.7	22

#	Article	IF	CITATIONS
559	Source contributions and spatiotemporal characteristics of PAHs in sediments: Using threeâ€way source apportionment approach. Environmental Toxicology and Chemistry, 2014, 33, 1747-1753.	4.3	12
560	Photodegradation of sulfapyridine under simulated sunlight irradiation: Kinetics, mechanism and toxicity evolvement. Chemosphere, 2014, 99, 186-191.	8.2	65
561	Vibration isolation via a scissor-like structured platform. Journal of Sound and Vibration, 2014, 333, 2404-2420.	3.9	162
562	Effects of Ce3+ doping concentrations on microstructure and luminescent properties of Ce3+:Lu3Al5O12 (Ce:LuAG) transparent ceramics. Optical Materials, 2014, 36, 1954-1958.	3.6	20
563	Historical trends of concentrations, source contributions and toxicities for PAHs in dated sediment cores from five lakes in western China. Science of the Total Environment, 2014, 470-471, 519-526.	8.0	61
564	A novel third chromosomal locus controls susceptibility to Autographa californica multiple nucleopolyhedrovirus in the silkworm, Bombyx mori. Applied Microbiology and Biotechnology, 2014, 98, 3049-3058.	3.6	5
565	Spatial and temporal distribution of polycyclic aromatic hydrocarbons (PAHs) in surface water from Liaohe River Basin, northeast China. Environmental Science and Pollution Research, 2014, 21, 7088-7096.	5.3	58
566	Establishment of Caenorhabditis elegans SID-1-Dependent DNA Delivery System in Cultured Silkworm Cells. Molecular Biotechnology, 2014, 56, 193-198.	2.4	9
567	Production of citric acid using its extraction wastewater treated by anaerobic digestion and ion exchange in an integrated citric acid-methane fermentation process. Bioprocess and Biosystems Engineering, 2014, 37, 1659-1668.	3.4	15
568	Complex dynamics in the Leslie–Gower type of the food chain system with multiple delays. Communications in Nonlinear Science and Numerical Simulation, 2014, 19, 2850-2865.	3.3	20
569	Bioaccumulation and trophic transfer of perfluorinated compounds in a eutrophic freshwater food web. Environmental Pollution, 2014, 184, 254-261.	7.5	113
570	Simultaneous quantification of several classes of antibiotics in water, sediments, and fish muscles by liquid chromatography-tandem mass spectrometry. Frontiers of Environmental Science and Engineering, 2014, 8, 357-371.	6.0	43
571	Stability and oscillations in a slow-fast flexible joint system with transformation delay. Acta Mechanica Sinica/Lixue Xuebao, 2014, 30, 727-738.	3.4	10
572	Occurrence, Distribution, Environmental Risk Assessment and Source Apportionment of Polycyclic Aromatic Hydrocarbons (PAHs) in Water and Sediments of the Liaohe River Basin, China. Bulletin of Environmental Contamination and Toxicology, 2014, 93, 744-751.	2.7	45
573	Occurrence, distribution and bioaccumulation of antibiotics in the Liao River Basin in China. Environmental Sciences: Processes and Impacts, 2014, 16, 586.	3.5	90
574	Dynamics of polycomb proteins-mediated histone modifications during UV irradiation-induced DNA damage. Insect Biochemistry and Molecular Biology, 2014, 55, 9-18.	2.7	9
575	Raman spectroscopy provides a rapid, nonâ€invasive method for quantitation of starch in live, unicellular microalgae. Biotechnology Journal, 2014, 9, 1512-1518.	3.5	50
576	Droplet breakup of micro- and nano-dispersed carbon-in-water colloidal suspensions under intense radiation. International Journal of Heat and Mass Transfer, 2014, 78, 267-276.	4.8	13

#	Article	IF	CITATIONS
577	Antagonistic roles of abscisic acid and cytokinin during response to nitrogen depletion in oleaginous microalga <i><scp>N</scp>annochloropsis oceanica</i> expand the evolutionary breadth of phytohormone function. Plant Journal, 2014, 80, 52-68.	5.7	101
578	Distribution, sources and composition of antibiotics in sediment, overlying water and pore water from Taihu Lake, China. Science of the Total Environment, 2014, 497-498, 267-273.	8.0	234
579	Scintillation and Luminescent Properties of Cerium Doped Lutetium Aluminum Garnet (Ce:LuAG) Powders and Transparent Ceramics. IEEE Transactions on Nuclear Science, 2014, 61, 373-379.	2.0	12
580	X-ray Absorption Fine Structure Analysis of Valence State of Ce in Polycrystalline Ce:LuAG Films. IEEE Transactions on Nuclear Science, 2014, 61, 428-432.	2.0	4
581	Lower temperature synthesis of cerium-doped polycrystalline lutetium pyrosilicate powders by a novel sol-gel processing. Science China Technological Sciences, 2014, 57, 1610-1615.	4.0	12
582	Effect of Acetic Acid on Citric Acid Fermentation in an Integrated Citric Acid–Methane Fermentation Process. Applied Biochemistry and Biotechnology, 2014, 174, 376-387.	2.9	2
583	Novel magnetically recoverable BiOBr/iron oxides heterojunction with enhanced visible light-driven photocatalytic activity. Applied Surface Science, 2014, 320, 383-390.	6.1	56
584	Femtosecond laser 3D micromachining: a powerful tool for the fabrication of microfluidic, optofluidic, and electrofluidic devices based on glass. Lab on A Chip, 2014, 14, 3447-3458.	6.0	190
585	Beneficial performance of a quasi-zero-stiffness vibration isolator with time-delayed active control. International Journal of Mechanical Sciences, 2014, 82, 32-40.	6.7	122
586	Species coexistence and chaotic behavior induced by multiple delays in a food chain system. Ecological Complexity, 2014, 19, 9-17.	2.9	32
587	Microwave-assisted conversion of microcrystalline cellulose to 5-hydroxymethylfurfural catalyzed by ionic liquids. Bioresource Technology, 2014, 162, 358-364.	9.6	62
588	A Quasi-Zero-Stiffness-Based Sensor System in Vibration Measurement. IEEE Transactions on Industrial Electronics, 2014, 61, 5606-5614.	7.9	29
589	Stability switches and Bogdanov-Takens bifurcation in an inertial two-neuron coupling system with multiple delays. Science China Technological Sciences, 2014, 57, 893-904.	4.0	44
590	Numerical Analysis on Effect of Areal Gas Distribution Pipe on Characteristics Inside COREX Shaft Furnace. Jom, 2014, 66, 1265-1276.	1.9	18
591	Expression, Purification, and Characterization of Endo-Î <sup>2</sup> -N-Acetylglucosaminidase H Using Baculovirus-Mediated Silkworm Protein Expression System. Applied Biochemistry and Biotechnology, 2014, 172, 3978-3988.	2.9	33
592	Analysis of vibration suppression of master structure in nonlinear systems using nonlinear delayed absorber. International Journal of Dynamics and Control, 2014, 2, 55-67.	2.5	5
593	Quantitative dynamics of triacylglycerol accumulation in microalgae populations at single-cell resolution revealed by Raman microspectroscopy. Biotechnology for Biofuels, 2014, 7, 58.	6.2	67
594	Regulation of the cholesterol biosynthetic pathway and its integration with fatty acid biosynthesis in the oleaginous microalga Nannochloropsis oceanica. Biotechnology for Biofuels, 2014, 7, 81.	6.2	81

#	Article	IF	CITATIONS
595	Baculovirus-mediated gene transfer systems in silkworm larvae using constitutive host promoters. Journal of Asia-Pacific Entomology, 2014, 17, 73-78.	0.9	1
596	Predictive modeling of gingivitis severity and susceptibility via oral microbiota. ISME Journal, 2014, 8, 1768-1780.	9.8	118
597	Chatter in a transverse grinding process. Journal of Sound and Vibration, 2014, 333, 937-953.	3.9	16
598	DNA Extraction Protocol for Biological Ingredient Analysis of Liuwei Dihuang Wan. Genomics, Proteomics and Bioinformatics, 2014, 12, 137-143.	6.9	26
599	Synthesis of BSO (Bi4Si3O12) scintillation thin film by sol–gel method. Journal of Alloys and Compounds, 2014, 582, 33-36.	5.5	14
600	Choreography of Transcriptomes and Lipidomes of <i>Nannochloropsis</i> Reveals the Mechanisms of Oil Synthesis in Microalgae Â. Plant Cell, 2014, 26, 1645-1665.	6.6	311
601	Distribution and ecological risk of antibiotics in a typical effluent–receiving river (Wangyang River) in north China. Chemosphere, 2014, 112, 267-274.	8.2	200
602	A conserved SUMOylation signaling for cell cycle control in a holocentric species Bombyx mori. Insect Biochemistry and Molecular Biology, 2014, 51, 71-79.	2.7	9
603	Fabrication and microstructure of cerium doped lutetium aluminum garnet (Ce:LuAC) transparent ceramics by solid-state reaction method. Materials Research Bulletin, 2014, 55, 161-167.	5.2	6
604	Delay-induced Hopf bifurcation in the double-link inverted pendulum system for human quiet standing. , 2014, , .		0
605	Genomic and transcriptome analyses reveal that MAPK- and phosphatidylinositol-signaling pathways mediate tolerance to 5-hydroxymethyl-2-furaldehyde for industrial yeast Saccharomyces cerevisiae. Scientific Reports, 2014, 4, 6556.	3.3	45
606	Biological ingredient analysis of traditional Chinese medicine preparation based on high-throughput sequencing: the story for Liuwei Dihuang Wan. Scientific Reports, 2014, 4, 5147.	3.3	132
607	Genome-wide identification of transcription factors and transcription-factor binding sites in oleaginous microalgae Nannochloropsis. Scientific Reports, 2014, 4, 5454.	3.3	75
608	Reduced Fetal Telomere Length in Gestational Diabetes. PLoS ONE, 2014, 9, e86161.	2.5	52
609	Parallel-META 2.0: Enhanced Metagenomic Data Analysis with Functional Annotation, High Performance Computing and Advanced Visualization. PLoS ONE, 2014, 9, e89323.	2.5	70
610	Development of HuMiChip for Functional Profiling of Human Microbiomes. PLoS ONE, 2014, 9, e90546.	2.5	18
611	QSpec: online control and data analysis system for single-cell Raman spectroscopy. PeerJ, 2014, 2, e436.	2.0	6
612	Structure and regulation of the cellulose degradome in Clostridium cellulolyticum. Biotechnology for Biofuels, 2013, 6, 73.	6.2	49

#	Article	IF	CITATIONS
613	Stability switches and double Hopf bifurcation in a two-neural network system with multiple delays. Cognitive Neurodynamics, 2013, 7, 505-521.	4.0	43
614	Fabrication, Microstructure, and Luminescent Properties of <scp><scp>Ce</scp></scp> 3+ â€Doped <scp><scp>Lu</scp></scp> <sub>3</sub> <scp><scp>Al</scp></scp> <sub>5</sub> <scp><scp>O</scp> (<scp><scp>Ce</scp></scp>:<scp>LuAG</scp></scp> ) Transparent Ceramics by Lowâ€Temperature Vacuum Sintering. Journal of the American Ceramic Society, 2013, 96, 1930-1936.	⇒ <su<b>abe&gt;12&lt;</su<b>	/sułta>
615	Pretreatment on Miscanthus lutarioriparious by liquid hot water for efficient ethanol production. Biotechnology for Biofuels, 2013, 6, 76.	6.2	70
616	Applications of the integral equation method to delay differential equations. Nonlinear Dynamics, 2013, 73, 2241-2260.	5.2	13
617	Removal of benzotriazole from solution by BiOBr photocatalysis under simulated solar irradiation. Chemical Engineering Journal, 2013, 221, 230-237.	12.7	95
618	Degradation of sulfonamides antibiotics in lake water and sediment. Environmental Science and Pollution Research, 2013, 20, 2372-2380.	5.3	79
619	Hopf bifurcation and chaos in an inertial neuron system with coupled delay. Science China Technological Sciences, 2013, 56, 2299-2309.	4.0	41
620	Removal of sulfadiazine from aqueous solution on kaolinite. Frontiers of Environmental Science and Engineering, 2013, 7, 836-843.	6.0	10
621	Adsorption of sulfonamides on lake sediments. Frontiers of Environmental Science and Engineering, 2013, 7, 518-525.	6.0	12
622	GPU-Meta-Storms: Computing the similarities among massive microbial communities using GPU. , 2013, , .		1
623	A new correction method for determination on carbohydrates in lignocellulosic biomass. Bioresource Technology, 2013, 138, 373-376.	9.6	29
624	Microevolution from shock to adaptation revealed strategies improving ethanol tolerance and production in Thermoanaerobacter. Biotechnology for Biofuels, 2013, 6, 103.	6.2	12
625	Nannochloropsis plastid and mitochondrial phylogenomes reveal organelle diversification mechanism and intragenus phylotyping strategy in microalgae. BMC Genomics, 2013, 14, 534.	2.8	55
626	Establishment of a soaking RNA interference and Bombyx mori nucleopolyhedrovirus (BmNPV)-hypersensitive cell line using Bme21 cell. Applied Microbiology and Biotechnology, 2013, 97, 10435-10444.	3.6	13
627	Photocatalytic degradation of carbamazepine by tailored BiPO4: efficiency, intermediates and pathway. Applied Catalysis B: Environmental, 2013, 130-131, 285-292.	20.2	129
628	The PathoChip, a functional gene array for assessing pathogenic properties of diverse microbial communities. ISME Journal, 2013, 7, 1974-1984.	9.8	32
629	Electrofluidics fabricated by space-selective metallization in glass microfluidic structures using femtosecond laser direct writing. Lab on A Chip, 2013, 13, 4608.	6.0	103
630	Production and characterization of the celery mismatch endonuclease CEL II using baculovirus/silkworm expression system. Applied Microbiology and Biotechnology, 2013, 97, 6813-6822.	3.6	13

#	Article	IF	CITATIONS
631	Fates and transport of PPCPs in soil receiving reclaimed water irrigation. Chemosphere, 2013, 93, 2621-2630.	8.2	88
632	Source apportionment of perfluorinated compounds (PFCs) in sediments: Using three multivariate factor analysis receptor models. Journal of Hazardous Materials, 2013, 260, 483-488.	12.4	31
633	DEM simulation of particle size segregation behavior during charging into and discharging from a Paul-Wurth type hopper. Chemical Engineering Science, 2013, 99, 314-323.	3.8	67
634	Stability switches and fold-Hopf bifurcations in an inertial four-neuron network model with coupling delay. Neurocomputing, 2013, 110, 70-79.	5.9	18
635	Multiphysics well-stirred reactor modeling of coal gasification under intense thermal radiation. International Journal of Hydrogen Energy, 2013, 38, 7007-7015.	7.1	3
636	Photodegradation of sulfamethazine in an aqueous solution by a bismuth molybdate photocatalyst. Catalysis Science and Technology, 2013, 3, 1603.	4.1	85
637	Soaking RNAi-mediated modification of Sf9 cells for baculovirus expression system by ectopic expression of Caenorhabditis elegans SID-1. Applied Microbiology and Biotechnology, 2013, 97, 5921-5931.	3.6	27
638	Dissecting and engineering metabolic and regulatory networks of thermophilic bacteria for biofuel production. Biotechnology Advances, 2013, 31, 827-837.	11.7	47
639	Characterization of Tudor-sn-containing granules in the silkworm, Bombyx mori. Insect Biochemistry and Molecular Biology, 2013, 43, 664-674.	2.7	14
640	Removal of rhodamine B from aqueous solution by BiPO4 hierarchical architecture. Frontiers of Environmental Science and Engineering, 2013, 7, 382-387.	6.0	12
641	AMINO ACID DEPRIVATIONâ€INDUCED EXPRESSION OF ASPARAGINE SYNTHETASE REGULATES THE GROWTH AND SURVIVAL OF CULTURED SILKWORM CELLS. Archives of Insect Biochemistry and Physiology, 2013, 83, 57-68.	1.5	1
642	Optimization of microwave-assisted calcium chloride pretreatment of corn stover. Bioresource Technology, 2013, 127, 112-118.	9.6	44
643	Quasiperiodic motion induced by heterogeneous delays in a simplified internet congestion control model. Nonlinear Analysis: Real World Applications, 2013, 14, 661-670.	1.7	9
644	Raman Activated Cell Ejection for Isolation of Single Cells. Analytical Chemistry, 2013, 85, 10697-10701.	6.5	105
645	Locomotion Gait Design of an Earthworm-Like Robot Based on Multi-Segment Fluidic Flexible Matrix Composite Structures. , 2013, , .		1
646	Absorption mechanism of the second pulse in double-pulse femtosecond laser glass microwelding. Optics Express, 2013, 21, 24049.	3.4	21
647	Delay Induced Strong and Weak Resonances in Delayed Differential Systems. , 2013, , 163-191.		0
648	Bifurcation Scenarios of Neural Firing Patterns across Two Separated Chaotic Regions as Indicated by Theoretical and Biological Experimental Models. Abstract and Applied Analysis, 2013, 2013, 1-12.	0.7	2

#	Article	IF	CITATIONS
649	Suppression of Regenerative Chatter in a Plunge-Grinding Process by Spindle Speed. Journal of Manufacturing Science and Engineering, Transactions of the ASME, 2013, 135, .	2.2	8
650	Application of Nakamura's Model to Describe the Delayed Increase in Lateral Vibration of Footbridges. Journal of Engineering Mechanics - ASCE, 2013, 139, 1708-1713.	2.9	4
651	Influence of the time delay of signal transmission on synchronization conditions in drive-response systems. Theoretical and Applied Mechanics Letters, 2013, 3, 063004.	2.8	2
652	STRONG AND WEAK RESONANCES IN DELAYED DIFFERENTIAL SYSTEMS. International Journal of Bifurcation and Chaos in Applied Sciences and Engineering, 2013, 23, 1350119.	1.7	9
653	Editorial: Dynamics on delayed systems. Theoretical and Applied Mechanics Letters, 2013, 3, 063001.	2.8	0
654	STABILITY AND HOPF BIFURCATION FOR A THREE-SPECIES REACTION–DIFFUSION PREDATOR–PREY SYSTEM WITH TWO DELAYS. International Journal of Bifurcation and Chaos in Applied Sciences and Engineering, 2013, 23, 1350194.	1.7	2
655	STABILITY SWITCH BOUNDARIES IN AN INTERNET CONGESTION CONTROL MODEL WITH DIVERSE TIME DELAYS. International Journal of Bifurcation and Chaos in Applied Sciences and Engineering, 2013, 23, 1330016.	1.7	7
656	Levels and distribution of tetrabromobisphenol A and hexabromocyclododecane in Taihu Lake, China. Environmental Toxicology and Chemistry, 2013, 32, 2249-2255.	4.3	60
657	QC-Chain: Fast and Holistic Quality Control Method for Next-Generation Sequencing Data. PLoS ONE, 2013, 8, e60234.	2.5	68
658	Numerical Analysis of the Characteristics Inside Pre-reduction Shaft Furnace and Its Operation Parameters Optimization by Using a Three-Dimensional Full Scale Mathematical Model. ISIJ International, 2013, 53, 576-582.	1.4	34
659	A Simple Approach to Achieve Modified Projective Synchronization between Two Different Chaotic Systems. Scientific World Journal, The, 2013, 2013, 1-7.	2.1	3
660	Cell Cycle-Dependent Recruitment of Polycomb Proteins to the ASNS Promoter Counteracts C/ebp-Mediated Transcriptional Activation in Bombyx mori. PLoS ONE, 2013, 8, e52320.	2.5	9
661	Root Development. , 2013, , 297-316.		1
662	Meta-Storms: efficient search for similar microbial communities based on a novel indexing scheme and similarity score for metagenomic data. Bioinformatics, 2012, 28, 2493-2501.	4.1	44
663	Suppressing Chatter in a Plunge Grinding Process: Application of Variable Rotational Speed of Workpiece. Applied Mechanics and Materials, 2012, 249-250, 259-262.	0.2	0
664	Stability Analysis of a Transverse Cylindrical Grinding Process. Advanced Materials Research, 2012, 479-481, 1190-1193.	0.3	0
665	Inphase and Antiphase Synchronization in a Delay-Coupled System With Applications to a Delay-Coupled FitzHugh–Nagumo System. IEEE Transactions on Neural Networks and Learning Systems, 2012, 23, 1659-1670.	11.3	36
666	WEAK RESONANT DOUBLE HOPF BIFURCATIONS IN AN INERTIAL FOUR-NEURON MODEL WITH TIME DELAY. International Journal of Neural Systems, 2012, 22, 63-75.	5.2	40

#	Article	IF	CITATIONS
667	BIFURCATION AND CHAOS ANALYSIS FOR A DELAYED TWO-NEURAL NETWORK WITH A VARIATION SLOPE RATIO IN THE ACTIVATION FUNCTION. International Journal of Bifurcation and Chaos in Applied Sciences and Engineering, 2012, 22, 1250105.	1.7	19
668	Development of Slope Stability Evaluation Process of Frozen Soil in Coupling Temperature Field. Advanced Materials Research, 2012, 446-449, 1948-1956.	0.3	0
669	SNP calling using genotype model selection on high-throughput sequencing data. Bioinformatics, 2012, 28, 643-650.	4.1	22
670	Bursting-like motion induced by time-varying delay in an internet congestion control model. Acta Mechanica Sinica/Lixue Xuebao, 2012, 28, 1169-1179.	3.4	3
671	Oxidative transformation of carbamazepine by manganese oxides. Environmental Science and Pollution Research, 2012, 19, 4206-4213.	5.3	26
672	Stability switches and multistability coexistence in a delay-coupled neural oscillators system. Journal of Theoretical Biology, 2012, 313, 98-114.	1.7	37
673	Molecular cloning of BmTUDOR-SN and analysis of its role in the RNAi pathway in the silkworm, Bombyx mori (Lepidoptera: Bombycidae). Applied Entomology and Zoology, 2012, 47, 207-215.	1.2	10
674	Characterization and mechanism of glass microwelding by double-pulse ultrafast laser irradiation. Optics Express, 2012, 20, 28893.	3.4	32
675	An analytic criterion for generalized synchronization in unidirectionally coupled systems based on the auxiliary system approach. Chaos, 2012, 22, 033146.	2.5	13
676	The Combination of High-Gain Sliding Mode Observers Used as Receivers in Secure Communication. IEEE Transactions on Circuits and Systems I: Regular Papers, 2012, 59, 2702-2712.	5.4	28
677	Hierarchical mesoporous TiO2 microspheres for the enhanced photocatalytic oxidation of sulfonamides and their mechanism. RSC Advances, 2012, 2, 4720.	3.6	32
678	Detailed numerical simulations of flame propagation in coal-dust clouds. Combustion Theory and Modelling, 2012, 16, 747-773.	1.9	7
679	Mathematical Modeling of Coal Gasification Processes in a Well-Stirred Reactor: Effects of Devolatilization and Moisture Content. Energy & amp; Fuels, 2012, 26, 5759-5768.	5.1	50
680	Potential source contributions and risk assessment of PAHs in sediments from Taihu Lake, China: Comparison of three receptor models. Water Research, 2012, 46, 3065-3073.	11.3	242
681	Saliva microbiomes distinguish caries-active from healthy human populations. ISME Journal, 2012, 6, 1-10.	9.8	320
682	Oscillatory dynamics induced by time delay in an internet congestion control model with ring topology. Applied Mathematics and Computation, 2012, 218, 11033-11041.	2.2	5
683	Analysis of YM-216391 Biosynthetic Gene Cluster and Improvement of the Cyclopeptide Production in a Heterologous Host. ACS Chemical Biology, 2012, 7, 646-651.	3.4	30
684	Microbial Community Changes Along a Land-Use Gradient of Desert Soil Origin. Pedosphere, 2012, 22, 593-603.	4.0	34

#	Article	IF	CITATIONS
685	Facile synthesis and photocatalytic application of hierarchical mesoporous Bi2MoO6 nanosheet-based microspheres. CrystEngComm, 2012, 14, 3602.	2.6	94
686	Structures and properties characterization of acrylonitrilebutadiene-styrene/organo-palygorskite clay composites. Journal Wuhan University of Technology, Materials Science Edition, 2012, 27, 1068-1071.	1.0	3
687	Performances of two biotrickling filters in treating H2S-containing waste gases and analysis of corresponding bacterial communities by pyrosequencing. Applied Microbiology and Biotechnology, 2012, 95, 1633-1641.	3.6	14
688	Distribution and Sources of Organochlorine Pesticides in Taihu Lake, China. Bulletin of Environmental Contamination and Toxicology, 2012, 89, 1235-1239.	2.7	23
689	A Culture-Independent Approach to Unravel Uncultured Bacteria and Functional Genes in a Complex Microbial Community. PLoS ONE, 2012, 7, e47530.	2.5	26
690	Genome-Wide Identification of Polycomb Target Genes Reveals a Functional Association of Pho with Scm in Bombyx mori. PLoS ONE, 2012, 7, e34330.	2.5	16
691	MetaSee: An Interactive and Extendable Visualization Toolbox for Metagenomic Sample Analysis and Comparison. PLoS ONE, 2012, 7, e48998.	2.5	14
692	Identification and characterization of Polycomb group genes in the silkworm, Bombyx mori. Molecular Biology Reports, 2012, 39, 5575-5588.	2.3	28
693	Nonlinear chatter with large amplitude in a cylindrical plunge grinding process. Nonlinear Dynamics, 2012, 69, 1781-1793.	5.2	20
694	Seasonal variations of concentrations, profiles and possible sources of polycyclic aromatic hydrocarbons in sediments from Taihu Lake, China. Journal of Soils and Sediments, 2012, 12, 933-941.	3.0	18
695	Sediment–pore water partition of PAH source contributions to the Yellow River using two receptor models. Journal of Soils and Sediments, 2012, 12, 1154-1163.	3.0	30
696	Ore-blending optimization model for sintering process based on characteristics of iron ores. International Journal of Minerals, Metallurgy and Materials, 2012, 19, 217-224.	4.9	30
697	Controlled motion of a two-module vibration-driven system induced by internal acceleration-controlled masses. Archive of Applied Mechanics, 2012, 82, 461-477.	2.2	25
698	Determination and partitioning behavior of perfluoroalkyl carboxylic acids and perfluorooctanesulfonate in water and sediment from Dianchi Lake, China. Chemosphere, 2012, 88, 1292-1299.	8.2	77
699	Multiphysics modeling of carbon gasification processes in a well-stirred reactor with detailed gas-phase chemistry. Combustion and Flame, 2012, 159, 1693-1707.	5.2	18
700	Single cell Raman spectroscopy for cell sorting and imaging. Current Opinion in Biotechnology, 2012, 23, 56-63.	6.6	180
701	Parallel-META: efficient metagenomic data analysis based on high-performance computation. BMC Systems Biology, 2012, 6, S16.	3.0	36
702	Photodegradation of four fluoroquinolone compounds by titanium dioxide under simulated solar light irradiation. Journal of Chemical Technology and Biotechnology, 2012, 87, 643-650.	3.2	57

#	Article	IF	CITATIONS
703	Codimension-two bursting analysis in the delayed neural system with external stimulations. Nonlinear Dynamics, 2012, 67, 309-328.	5.2	58
704	Dynamics of a three-module vibration-driven system with non-symmetric Coulomb's dry friction. Multibody System Dynamics, 2012, 27, 455-485.	2.7	31
705	Bar-Coded Pyrosequencing Reveals the Responses of PBDE-Degrading Microbial Communities to Electron Donor Amendments. PLoS ONE, 2012, 7, e30439.	2.5	43
706	Metagenomic Insights into the Fibrolytic Microbiome in Yak Rumen. PLoS ONE, 2012, 7, e40430.	2.5	98
707	Indonesian Throughflow variability during the last 140 ka: the Timor Sea outflow. Geological Society Special Publication, 2011, 355, 283-303.	1.3	36
708	Establishing Oleaginous Microalgae Research Models for Consolidated Bioprocessing of Solar Energy. Advances in Biochemical Engineering/Biotechnology, 2011, 128, 69-84.	1.1	21
709	Bifurcation, amplitude death and oscillation patterns in a system of three coupled van der Pol oscillators with diffusively delayed velocity coupling. Chaos, 2011, 21, 023111.	2.5	28
710	Prediction of Pre-reduction Shaft Furnace with Top Gas Recycling Technology Aiming to Cut Down CO2 Emission. ISIJ International, 2011, 51, 1344-1352.	1.4	27
711	Autotrophic growth of nitrifying community in an agricultural soil. ISME Journal, 2011, 5, 1226-1236.	9.8	366
712	Photocatalytic degradation of tetrabromobisphenol A by mesoporous BiOBr: Efficacy, products and pathway. Applied Catalysis B: Environmental, 2011, 107, 355-362.	20.2	270
713	Optimization of microwave pretreatment on wheat straw for ethanol production. Biomass and Bioenergy, 2011, 35, 3859-3864.	5.7	71
714	Photoactivated Green Fluorescence Emission by Femtosecond Oscillator from Indole Solutions. Journal of Fluorescence, 2011, 21, 2185-2191.	2.5	0
715	Multiple scales analysis for double Hopf bifurcation withÂ1:3Âresonance. Nonlinear Dynamics, 2011, 66, 39-51.	5.2	21
716	Spatial Distribution of Polycyclic Aromatic Hydrocarbons from Lake Taihu, China. Bulletin of Environmental Contamination and Toxicology, 2011, 87, 80-85.	2.7	29
717	A deteriorating system with its repairman having multiple vacations. Applied Mathematics and Computation, 2011, 217, 4980-4989.	2.2	39
718	Oscillation control for n-dimensional congestion control model via time-varying delay. Science China Technological Sciences, 2011, 54, 2044-2053.	4.0	9
719	Preliminary characterization of the oral microbiota of Chinese adults with and without gingivitis. BMC Oral Health, 2011, 11, 33.	2.3	104
720	Circumferential burden distribution behaviors at bell-less top blast furnace with parallel type hoppers. Applied Mathematical Modelling, 2011, 35, 1439-1455.	4.2	41

#	Article	IF	CITATIONS
721	Photodegradation of rhodamine B and methyl orange over one-dimensional TiO2 catalysts under simulated solar irradiation. Applied Surface Science, 2011, 257, 3798-3803.	6.1	104
722	Dynamics of a mobile system with an internal acceleration-controlled mass in a resistive medium. Journal of Sound and Vibration, 2011, 330, 4002-4018.	3.9	46
723	Synchronization and synchronized periodic solution in a simplified five-neuron BAM neural network with delays. Neurocomputing, 2011, 74, 993-999.	5.9	22
724	An optimal replacement policy for a repairable system based on its repairman having vacations. Reliability Engineering and System Safety, 2011, 96, 868-875.	8.9	39
725	Adsorption of Aniline from Aqueous Solution by KSF Montmorillonite. Advanced Materials Research, 2011, 356-360, 208-216.	0.3	Ο
726	Adsorption of Phenol on Natural Sediment from Liaohe River, China. Advanced Materials Research, 2011, 356-360, 252-258.	0.3	0
727	Correlation of Genomic and Physiological Traits of Thermoanaerobacter Species with Biofuel Yields. Applied and Environmental Microbiology, 2011, 77, 7998-8008.	3.1	42
728	AN EFFICIENT METHOD FOR STUDYING FOLD-HOPF BIFURCATION IN DELAYED NEURAL NETWORKS. International Journal of Bifurcation and Chaos in Applied Sciences and Engineering, 2011, 21, 1393-1406.	1.7	9
729	The Thermoanaerobacter Glycobiome Reveals Mechanisms of Pentose and Hexose Co-Utilization in Bacteria. PLoS Genetics, 2011, 7, e1002318.	3.5	37
730	Time-varying delayed feedback control for an internet congestion control model. Discrete and Continuous Dynamical Systems - Series B, 2011, 16, 653-668.	0.9	8
731	Thermal regime of a thermokarst lake and its influence on permafrost, Beiluhe Basin, Qinghaiâ€Tibet Plateau. Permafrost and Periglacial Processes, 2010, 21, 315-324.	3.4	96
732	Investigation of acetic acid-catalyzed hydrothermal pretreatment on corn stover. Applied Microbiology and Biotechnology, 2010, 86, 509-516.	3.6	27
733	Spatial and Temporal Variations of Heavy Metals in Surface Sediments in Bohai Bay, North China. Bulletin of Environmental Contamination and Toxicology, 2010, 84, 482-487.	2.7	56
734	Ore-proportioning optimization technique with high proportion of Yandi ore in sintering. International Journal of Minerals, Metallurgy and Materials, 2010, 17, 11-16.	4.9	13
735	Fold-Hopf bifurcation in a simplified four-neuron BAM (bidirectional associative memory) neural network with two delays. Science China Technological Sciences, 2010, 53, 633-644.	4.0	16
736	Feasibility of Hydrothermal Pretreatment on Maize Silage for Bioethanol Production. Applied Biochemistry and Biotechnology, 2010, 162, 33-42.	2.9	27
737	Delayed saturation controller for vibration suppression inÂaÂstainless-steel beam. Nonlinear Dynamics, 2010, 62, 177-193.	5.2	28
738	Simple zero singularity analysis in a coupled FitzHugh–Nagumo neural system with delay. Neurocomputing, 2010, 73, 874-882.	5.9	26

#	Article	IF	CITATIONS
739	Leaching potential of nonsteroidal antiâ€inflammatory drugs in soils. Environmental Toxicology and Chemistry, 2010, 29, 800-807.	4.3	30
740	Application of the Cluster–Cluster Aggregation model to an open system. Journal of Colloid and Interface Science, 2010, 344, 37-43.	9.4	16
741	Impact of long-term reclaimed wastewater irrigation on agricultural soils: A preliminary assessment. Journal of Hazardous Materials, 2010, 183, 780-786.	12.4	174
742	Effects of technological delay on insulin and blood glucose in a physiological model. International Journal of Non-Linear Mechanics, 2010, 45, 628-633.	2.6	4
743	Factors influencing cellulosome activity in Consolidated Bioprocessing of cellulosic ethanol. Bioresource Technology, 2010, 101, 9560-9569.	9.6	54
744	Projective synchronization of different chaotic time-delayed neural networks based on integral sliding mode controller. Applied Mathematics and Computation, 2010, 217, 164-174.	2.2	81
745	Ethanol production from hydrothermal pretreated corn stover with a loop reactor. Biomass and Bioenergy, 2010, 34, 334-339.	5.7	24
746	Bautin bifurcation analysis for synchronous solution of a coupled FHN neural system with delay. Communications in Nonlinear Science and Numerical Simulation, 2010, 15, 442-458.	3.3	24
747	Basic Characteristics of the Shaft Furnace of COREX® Smelting Reduction Process Based on Iron Oxides Reduction Simulation. ISIJ International, 2010, 50, 1032-1039.	1.4	50
748	THEORETICAL STUDY ON METHANE HYDROXYLATION BY MIMIC METHANE MONOOXYGENASE WITH bis(μ-OXO)DIMANGANESE CORE. Journal of Theoretical and Computational Chemistry, 2010, 09, 233-247.	1.8	1
749	Setting position of bus station on expressway. , 2010, , .		0
750	FOLD–HOPF BIFURCATION ANALYSIS FOR A COUPLED FITZHUGH–NAGUMO NEURAL SYSTEM WITH TIME DELAY. International Journal of Bifurcation and Chaos in Applied Sciences and Engineering, 2010, 20, 3919-3934.	1.7	32
751	Factors contributing to urban expressway entrance and exit safety. , 2010, , .		2
752	Effects of Time Delay and Noise on Asymptotic Stability in Human Quiet Standing Model. Mathematical Problems in Engineering, 2010, 2010, 1-14.	1.1	4
753	Simultaneous Formation of Two types of Periodic Nanostructure in ZnO Single Crystal by Femtosecond Laser Direct Irradiation. Japanese Journal of Applied Physics, 2010, 49, 112001.	1.5	1
754	Surface-Enhanced Raman Scattering Substrate Fabricated by Femtosecond Laser Induced Co-deposition of Silver Nanoparticles and Fluorescent Molecules. Japanese Journal of Applied Physics, 2010, 49, 022703.	1.5	6
755	Indo-Pacific Warm Pool variability during the Holocene and Last Glacial Maximum. Paleoceanography, 2010, 25, n/a-n/a.	3.0	48
756	Computation of Synchronized Periodic Solution in a BAM Network With Two Delays. IEEE Transactions on Neural Networks, 2010, 21, 439-450.	4.2	19

#	Article	IF	CITATIONS
757	Redistribution of elements in glass induced by a high-repetition-rate femtosecond laser. Optics Express, 2010, 18, 6262.	3.4	35
758	Direct fabrication of homogeneous microfluidic channels embedded in fused silica using a femtosecond laser. Optics Letters, 2010, 35, 282.	3.3	75
759	Ultrasound-Mediated DNA Transformation in Thermophilic Gram-Positive Anaerobes. PLoS ONE, 2010, 5, e12582.	2.5	36
760	Outer synchronization of coupled discrete-time networks. Chaos, 2009, 19, 013106.	2.5	98
761	Optimal control for a class of hybrid systems in manufacturing. , 2009, , .		0
762	Characterization of the Central Metabolic Pathways in <i>Thermoanaerobacter</i> sp. Strain X514 via Isotopomer-Assisted Metabolite Analysis. Applied and Environmental Microbiology, 2009, 75, 5001-5008.	3.1	57
763	BURSTING NEAR BAUTIN BIFURCATION IN A NEURAL NETWORK WITH DELAY COUPLING. International Journal of Neural Systems, 2009, 19, 359-373.	5.2	24
764	Novel Features of the Polysaccharide-Digesting Gliding Bacterium <i>Flavobacterium johnsoniae</i> as Revealed by Genome Sequence Analysis. Applied and Environmental Microbiology, 2009, 75, 6864-6875.	3.1	212
765	A perturbation-incremental scheme for studying Hopf bifurcation in delayed differential systems. Science in China Series D: Earth Sciences, 2009, 52, 698-708.	0.9	28
766	Heavy Metals in the Surface Sediments in Lanzhou Reach of Yellow River, China. Bulletin of Environmental Contamination and Toxicology, 2009, 82, 26-30.	2.7	103
767	Decennary Variations of Dissolved Heavy Metals in Seawater of Bohai Bay, North China. Bulletin of Environmental Contamination and Toxicology, 2009, 83, 907-912.	2.7	21
768	Rapid fabrication of optical volume gratings in Foturan glass byÂfemtosecond laser micromachining. Applied Physics A: Materials Science and Processing, 2009, 97, 853-857.	2.3	22
769	Fabrication of an integrated Raman sensor by selective surface metallization using a femtosecond laser oscillator. Optics Communications, 2009, 282, 1370-1373.	2.1	12
770	Recovery of arabinan in acetic acid-catalyzed hydrothermal pretreatment on corn stover. Biomass and Bioenergy, 2009, 33, 1660-1663.	5.7	9
771	Simulation of the spectra and determination of the optical constants of online low-emission glass from visible to mid-infrared region. Thin Solid Films, 2009, 517, 2963-2967.	1.8	6
772	First principle study on the electronic structure of fluorine-doped SnO2. Solid State Communications, 2009, 149, 527-531.	1.9	62
773	Sediment-porewater partition of polycyclic aromatic hydrocarbons (PAHs) from Lanzhou Reach of Yellow River, China. Journal of Hazardous Materials, 2009, 165, 494-500.	12.4	64
774	Enzymatic hydrolysis and fermentability of corn stover pretreated by lactic acid and/or acetic acid. Journal of Biotechnology, 2009, 139, 300-305.	3.8	51

#	Article	IF	CITATIONS
775	Optimization of ethanol production from hot-water extracts of sugar maple chips. Renewable Energy, 2009, 34, 2353-2356.	8.9	8
776	Dynamics for a class of nonlinear systems with time delay. Chaos, Solitons and Fractals, 2009, 40, 28-49.	5.1	27
777	Delayed feedbacks to control the fractal erosion of safe basins in a parametrically excited system. Chaos, Solitons and Fractals, 2009, 41, 1880-1896.	5.1	28
778	Local and global bifurcations in an SIRS epidemic model. Applied Mathematics and Computation, 2009, 214, 534-547.	2.2	6
779	Leachability of some emerging contaminants in reclaimed municipal wastewaterâ€irrigated turf grass fields. Environmental Toxicology and Chemistry, 2009, 28, 1842-1850.	4.3	67
780	Modeling and optimal control of automated trolleys. , 2009, , .		1
781	Degradation and adsorption of selected pharmaceuticals and personal care products (PPCPs) in agricultural soils. Chemosphere, 2009, 77, 1299-1305.	8.2	300
782	Chaotic and Hyperchaotic Attractors in Time-Delayed Neural Networks. Lecture Notes of the Institute for Computer Sciences, Social-Informatics and Telecommunications Engineering, 2009, , 1193-1202.	0.3	4
783	Pharmaceuticals and Personal Care Products (PPCPs), and Endocrine Disrupting Compounds (EDCs) in Runoff from a Potato Field Irrigated with Treated Wastewater in Southern California. Journal of Health Science, 2009, 55, 306-310.	0.9	27
784	Adsorption and Degradation of Ketoprofen in Soils. Journal of Environmental Quality, 2009, 38, 1177-1182.	2.0	54
785	Delay-Induced Hopf Bifurcation and Periodic Solution in a BAM Network with Two Delays. Lecture Notes in Computer Science, 2009, , 534-543.	1.3	0
786	Fabrication of microelectrodes deeply embedded in LiNbO3 using a femtosecond laser. Applied Surface Science, 2008, 254, 7018-7021.	6.1	29
787	Simultaneous saccharification and fermentation of steam exploded wheat straw pretreated with alkaline peroxide. Process Biochemistry, 2008, 43, 1462-1466.	3.7	124
788	Determination of optical constants of functional layer of online Low-E glass based on the Drude theory. Thin Solid Films, 2008, 516, 3179-3183.	1.8	31
789	Sediment–Porewater Partition of Nonylphenol Polyethoxylates: Field Measurements from Lanzhou Reach of Yellow River, China. Archives of Environmental Contamination and Toxicology, 2008, 55, 173-179.	4.1	11
790	A kinetic spectrophotometric method for the determination of iron (III) in water samples. Journal of Ocean University of China, 2008, 7, 161-165.	1.2	5
791	Simultaneous determination of pharmaceuticals, endocrine disrupting compounds and hormone in soils by gas chromatography–mass spectrometry. Journal of Chromatography A, 2008, 1202, 189-195.	3.7	136
792	Simultaneous three-photon absorption induced ultraviolet upconversion in Pr3+:Y2SiO5 crystal by femtosecond laser irradiation. Optics Communications, 2008, 281, 299-302.	2.1	12

#	Article	IF	CITATIONS
793	Mechanism study of femtosecond laser induced selective metallization (FLISM) on glass surfaces. Optics Communications, 2008, 281, 3505-3509.	2.1	9
794	Electro-optic integration of embedded electrodes and waveguides in LiNbO_3 using a femtosecond laser. Optics Letters, 2008, 33, 2281.	3.3	88
795	Changes in the thermocline structure of the Indonesian outflow during Terminations I and II. Earth and Planetary Science Letters, 2008, 273, 152-162.	4.4	120
796	Dynamics of multi-rigid-body systems under non-smooth constraints and linear complementary problems. International Journal of Computer Mathematics, 2008, 85, 889-898.	1.8	3
797	Local and Global Existences of Synchronized Periodic Solutions in a Tri-neuron Network Model with Delay. , 2008, , .		0
798	Growth of single-crystalline tungsten nanowires by an alloy-catalyzed method at 850 °C. Journal of Materials Research, 2008, 23, 72-77.	2.6	11
799	Surface-Enhanced Raman Scattering Substrate Fabricated by Femtosecond Laser Direct Writing. Japanese Journal of Applied Physics, 2008, 47, 189-192.	1.5	28
800	Microstructures induced in the bulk of SrTiO3 crystal by a femtosecond laser. Optics Express, 2007, 15, 2341.	3.4	13
801	Selective metallization on insulator surfaces with femtosecond laser pulses. Optics Express, 2007, 15, 12743.	3.4	67
802	Orientation-controllable self-organized microgratings induced in the bulk SrTiO_3 crystal by a single femtosecond laser beam. Optics Express, 2007, 15, 14524.	3.4	13
803	Polycyclic aromatic hydrocarbons in the surface sediments from Yellow River, China. Chemosphere, 2007, 67, 1408-1414.	8.2	137
804	An Efficient Method for Studying Weak Resonant Double Hopf Bifurcation in Nonlinear Systems with Delayed Feedbacks. SIAM Journal on Applied Dynamical Systems, 2007, 6, 29-60.	1.6	81
805	Evolution of Symbiotic Bacteria in the Distal Human Intestine. PLoS Biology, 2007, 5, e156.	5.6	490
806	Upconversion luminescence and optical power limiting effect based on two- and three-photon absorption processes of ZnO crystal. Optics Communications, 2007, 280, 197-201.	2.1	15
807	Effects of delayed feedback control on nonlinear vibration absorber system. Journal of Sound and Vibration, 2007, 308, 212-230.	3.9	105
808	Synthesis of single-crystalline tungsten nanowires by nickel-catalyzed vapor-phase method at 850°C. Journal of Crystal Growth, 2007, 306, 433-436.	1.5	31
809	Standing electron plasma wave mechanism of void array formation inside glass by femtosecond laser irradiation. Applied Physics A: Materials Science and Processing, 2007, 88, 285-288.	2.3	18
810	Sliding state stepping algorithm for solving impact problems of multi-rigid-body system with joint friction. Applied Mathematics and Mechanics (English Edition), 2007, 28, 1621-1627.	3.6	3

#	Article	IF	CITATIONS
811	A Novel Stepwise Recovery Strategy of Cellulase Adsorbed to the Residual Substrate after Hydrolysis of Steam Exploded Wheat Straw. Applied Biochemistry and Biotechnology, 2007, 143, 93-100.	2.9	6
812	Changes in the vertical profile of the Indonesian Throughflow during Termination II: Evidence from the Timor Sea. Paleoceanography, 2006, 21, .	3.0	56
813	Effect of surfactants on desorption of aldicarb from spiked soil. Chemosphere, 2006, 62, 1630-1635.	8.2	26
814	Ionic liquid-containing semipermeable membrane devices for monitoring the polycyclic aromatic hydrocarbons in water. Chemosphere, 2006, 62, 1623-1629.	8.2	14
815	Seasonal and spatial distribution of nonylphenol in Lanzhou Reach of Yellow River in China. Chemosphere, 2006, 65, 1445-1451.	8.2	71
816	Distribution and dissipation pathways of nonylphenol polyethoxylates in the Yellow River: Site investigation and lab-scale studies. Environment International, 2006, 32, 907-914.	10.0	25
817	Lyapunov stability for a class of predator–prey model with delayed nutrient recycling. Chaos, Solitons and Fractals, 2006, 28, 173-181.	5.1	2
818	Flow-induced internal resonances and mode exchange in horizontal cantilevered pipe conveying fluid (I). Applied Mathematics and Mechanics (English Edition), 2006, 27, 935-941.	3.6	23
819	Flow-induced internal resonances and mode exchange in horizontal cantilevered pipe conveying fluid (II). Applied Mathematics and Mechanics (English Edition), 2006, 27, 943-951.	3.6	18
820	Leaching of Copper from an Industrial Sludge Applied on a Soil Column. Bulletin of Environmental Contamination and Toxicology, 2006, 76, 663-670.	2.7	1
821	Preparation of microspheres with silicone oil cores and poly(N-isopropylacrylamide) shells by physical coating. Journal of Applied Polymer Science, 2006, 102, 5571-5576.	2.6	2
822	Identification of genes subject to positive selection in uropathogenic strains of Escherichia coli: A comparative genomics approach. Proceedings of the National Academy of Sciences of the United States of America, 2006, 103, 5977-5982.	7.1	509
823	The complete genome sequence of a chronic atrophic gastritis Helicobacter pylori strain: Evolution during disease progression. Proceedings of the National Academy of Sciences of the United States of America, 2006, 103, 9999-10004.	7.1	228
824	Temperature control at different bed depths in a novel solid-state fermentation system with two dynamic changes of air. Biochemical Engineering Journal, 2005, 23, 117-122.	3.6	49
825	Investigating hookworm genomes by comparative analysis of two Ancylostoma species. BMC Genomics, 2005, 6, 58.	2.8	47
826	Leaching Behavior of Copper (II) in a Soil Column Experiment. Bulletin of Environmental Contamination and Toxicology, 2005, 75, 1028-1033.	2.7	3
827	Classification and Computation of Non-resonant Double Hopf Bifurcations and Solutions in Delayed van der Pol-Duffing System. International Journal of Nonlinear Sciences and Numerical Simulation, 2005, 6, .	1.0	10
828	MapLinker: a software tool that aids physical map-linked whole genome shotgun assembly. Bioinformatics, 2005, 21, 1265-1266.	4.1	4

#	Article	IF	CITATIONS
829	An integrated functional genomics and metabolomics approach for defining poor prognosis in human neuroendocrine cancers. Proceedings of the National Academy of Sciences of the United States of America, 2005, 102, 9901-9906.	7.1	102
830	Glycan Foraging in Vivo by an Intestine-Adapted Bacterial Symbiont. Science, 2005, 307, 1955-1959.	12.6	1,000
831	Fosmid-Based Physical Mapping of the Histoplasma capsulatum Genome. Genome Research, 2004, 14, 1603-1609.	5.5	23
832	DELAY-INDUCED BIFURCATIONS IN A NONAUTONOMOUS SYSTEM WITH DELAYED VELOCITY FEEDBACKS. International Journal of Bifurcation and Chaos in Applied Sciences and Engineering, 2004, 14, 2777-2798.	1.7	59
833	Message from a human gut symbiont: sensitivity is a prerequisite for sharing. Trends in Microbiology, 2004, 12, 21-28.	7.7	87
834	Plant uptake of aldicarb from contaminated soil and its enhanced degradation in the rhizosphere. Chemosphere, 2004, 54, 569-574.	8.2	55
835	A Genomic View of the Human- <i>Bacteroides thetaiotaomicron</i> Symbiosis. Science, 2003, 299, 2074-2076.	12.6	1,186
836	Honor thy symbionts. Proceedings of the National Academy of Sciences of the United States of America, 2003, 100, 10452-10459.	7.1	795
837	Neogene oxygen isotopic stratigraphy, ODP Site 1148, northern South China Sea. Science in China Series D: Earth Sciences, 2001, 44, 934-942.	0.9	42
838	A record of Miocene carbon excursions in the South China Sea. Science in China Series D: Earth Sciences, 2001, 44, 943-951.	0.9	26
839	Title is missing!. Applied Mathematics and Mechanics (English Edition), 2001, 22, 972-982.	3.6	1
840	Local bifurcation theory of nonlinear systems with parametric excitation. Nonlinear Dynamics, 1996, 10, 203-220.	5.2	3
841	Synthesis of γ-Bi <sub>2</sub> MoO <sub>6</sub> Spheres and their Photocatalytic Activities for Degradation of Rhodamine B. Advanced Materials Research, 0, 476-478, 988-993.	0.3	1
842	Ultrasonic Assisted Dynamic Inverse Emulsion: A Novel Polymerization Technique to Prepare Conductive Polyaniline/Palygorskite Composite. Advanced Materials Research, 0, 873, 507-513.	0.3	0
843	Do shareholders tolerate faults in scientific and technological innovation? Evidence from Chinese listed companies. Technology Analysis and Strategic Management, 0, , 1-13.	3.5	0
844	Coordinated optimization of locomotion velocity and energy consumption in vibration-driven system. Meccanica, 0, , 1.	2.0	2
845	<i>In vivo</i> enzymatic digestion of HRV 3C protease cleavage sites-containing proteins produced in a silkworm-baculovirus expression system. Bioscience Reports, 0, , .	2.4	3